Kinetics of Non-Thermal Atmospheric Pressure Plasmas

Alexander Fridman

- **Microdischarge Interaction and Structuring in Dielectric Barrier Discharges**
- **Kinetics of Blood Coagulation in Plasma**
- **Surface Wound Sterilization Kinetics**

Princeton, 2005

Microdischarge Interaction and Structuring in Dielectric Barrier Discharges

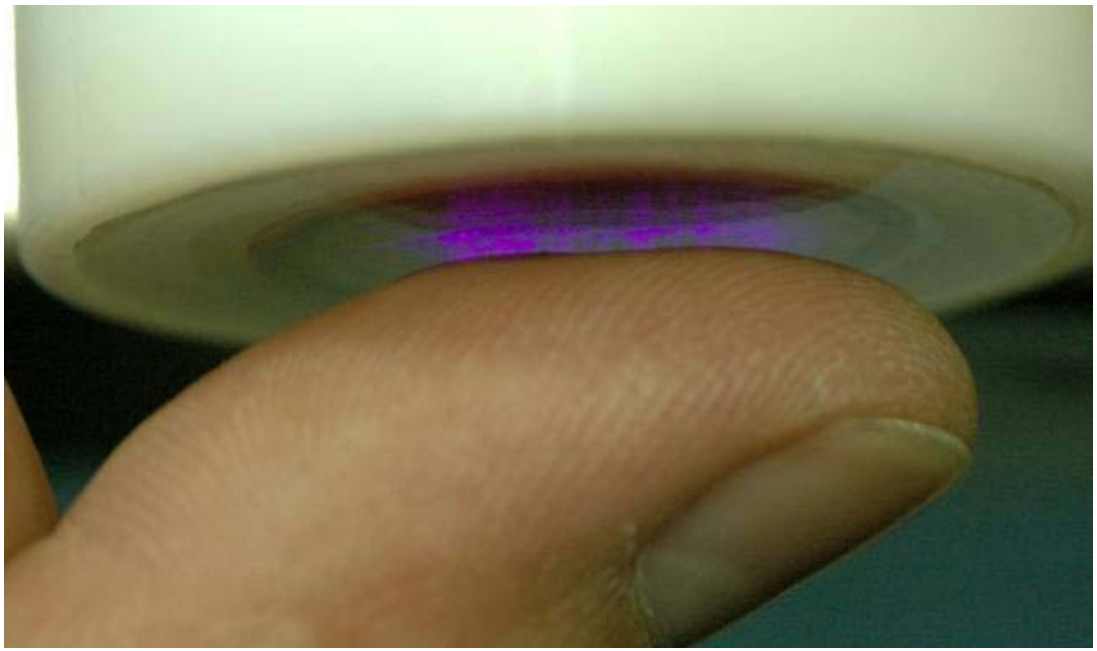

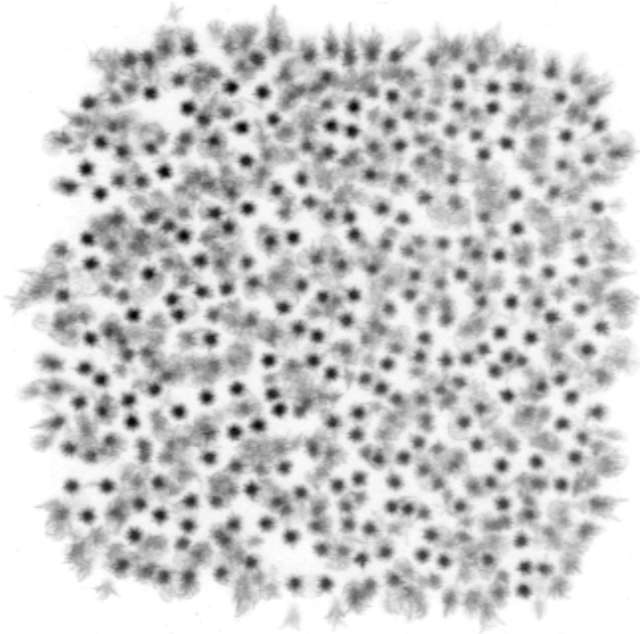

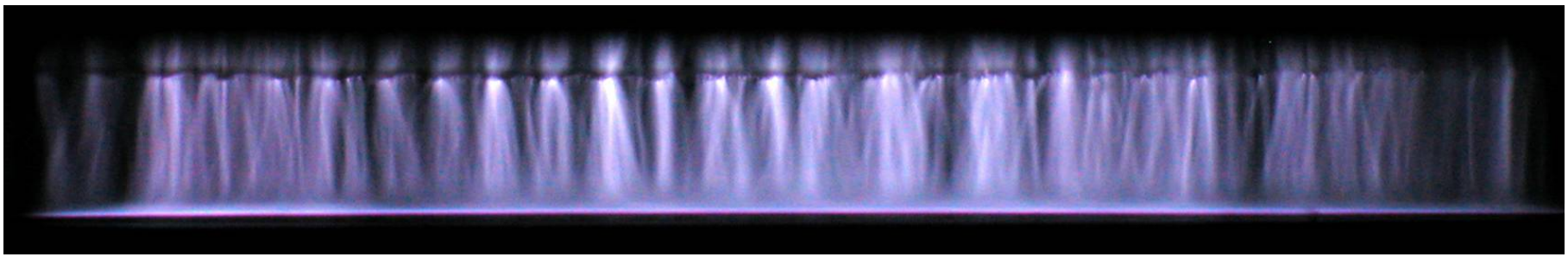

Formation of Microdischarges in DBD

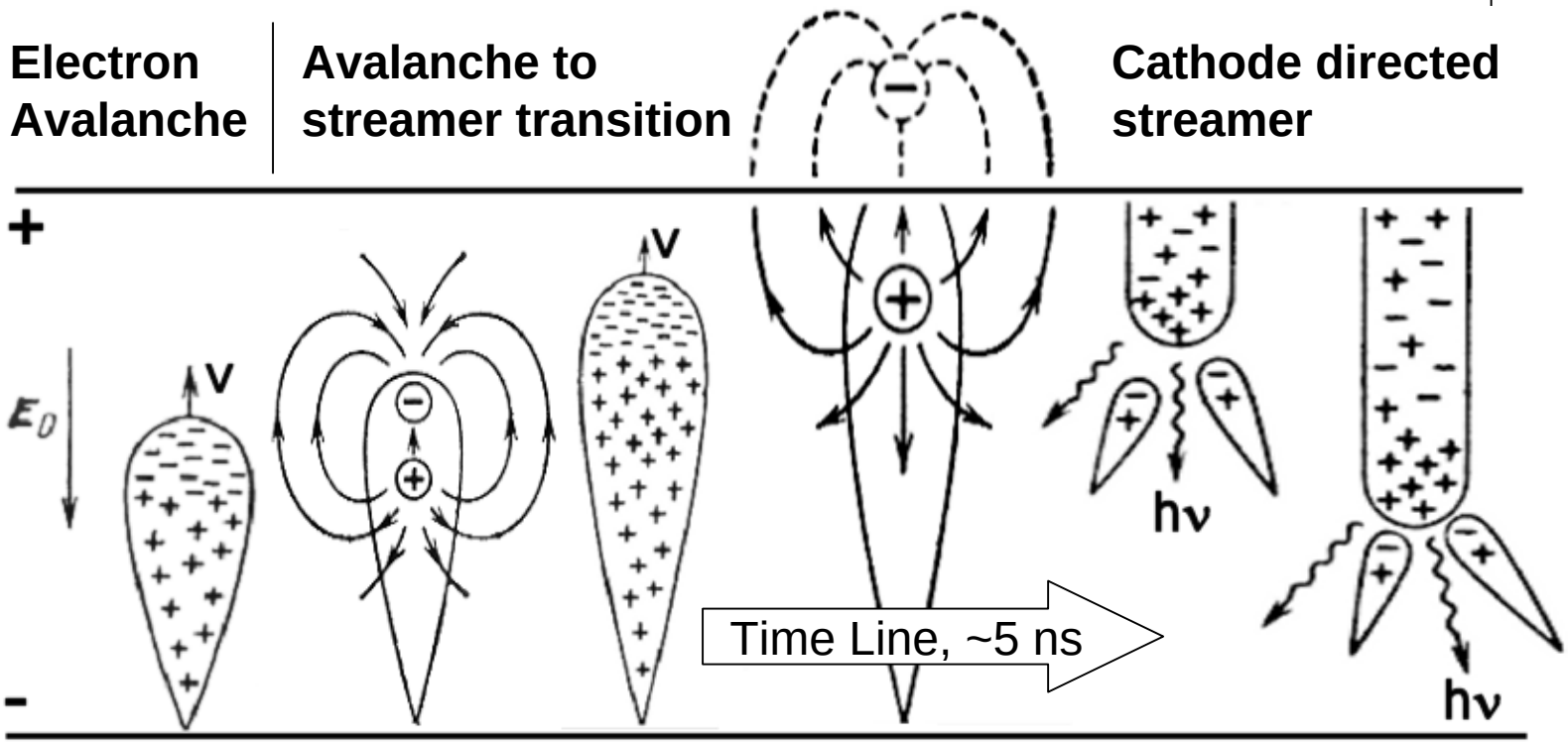

Avalanche =>

Streamer =>

Microdischarge

Duration	1-10 ns	Energy	10^{-7} 10^{-6} J
Radius	0.1 mm	Electron Energy	1-10 eV
Peak Current	0.1 A		
Current Density	10^{2}-10^{3} A/cm2	Electron Density	10^{14}-10^{15} 1/cm3
Total Charge	10^{-10} 10^{-9} C		

Avalanche to Streamer Transition (2D)

System of PDEs that describes avalanches and streamers in DBD

$$\frac{\partial N_e}{\partial t} = S + N_e\alpha\cdot|W_e| - N_e\eta\cdot|W_e| - N_eN_p\beta + div\,(D\cdot grad\,(N_e) - N_eW_e)$$

$$\frac{\partial N_p}{\partial t} = S + N_e\alpha\cdot|W_e| - N_eN_p\beta - N_nN_p\beta - div(N_pW_p)$$

$$\frac{\partial N_n}{\partial t} = N_e\eta\cdot|W_e| - N_nN_p\beta - div(N_nW_n)$$

$$\nabla^2\phi = -\frac{e}{\varepsilon}(N_p - N_e - N_n)$$

$$E = -\nabla\phi$$

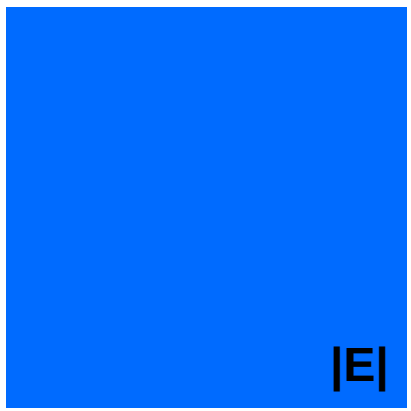

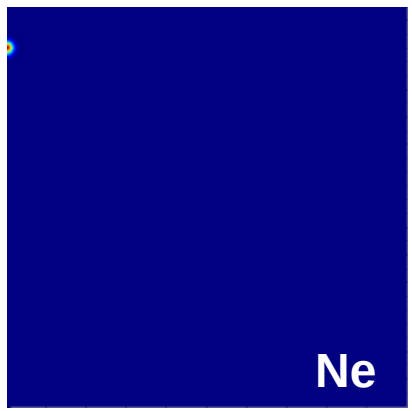

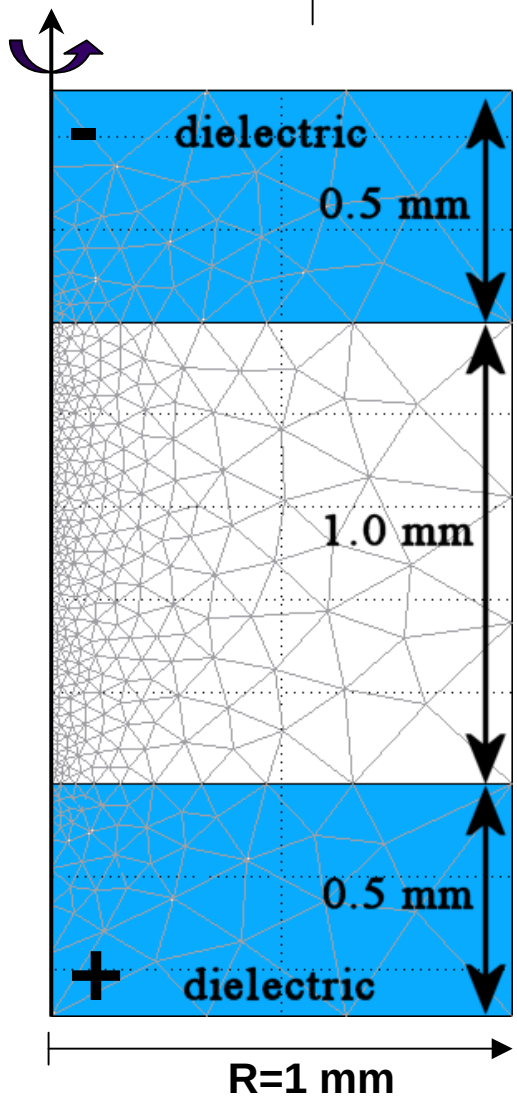

Microdischarge Interaction

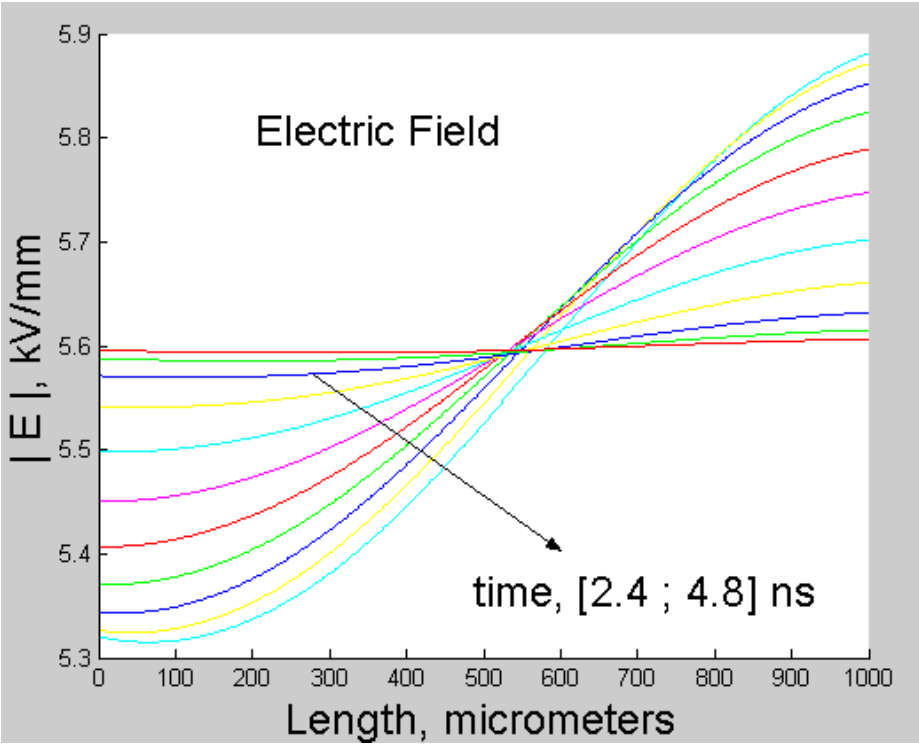

Repulsion

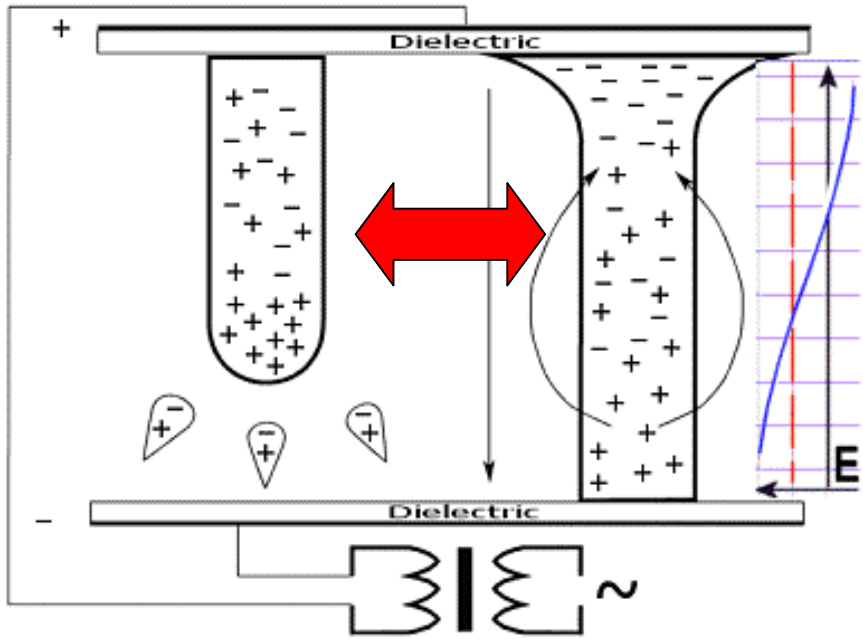

Effect of streamer space charge.

- **Decrease of |E| near Anode**
- **Increase of |E| near Cathode**

Formation of nearby streamers is suppressed.

Microdischarge Interaction (1D)

Maximum Voltage: 18.4 kV
Operating Frequency: 6.8 kHz
Power Consumption: ~100 Watts

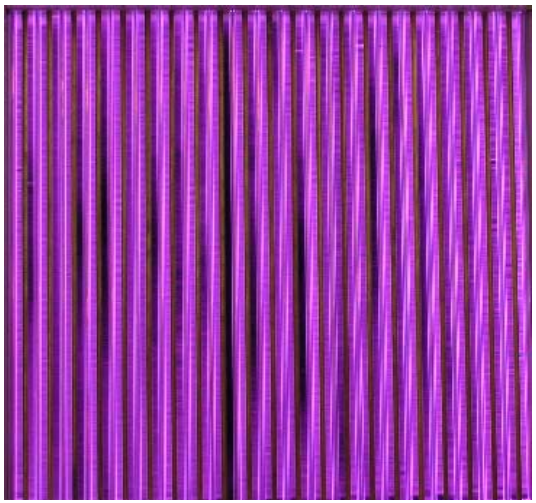

150 cm (6.5”)

Area of DBD plasma region: ~104cm^2

Quartz Capillary covers high voltage wire

30 frames per second

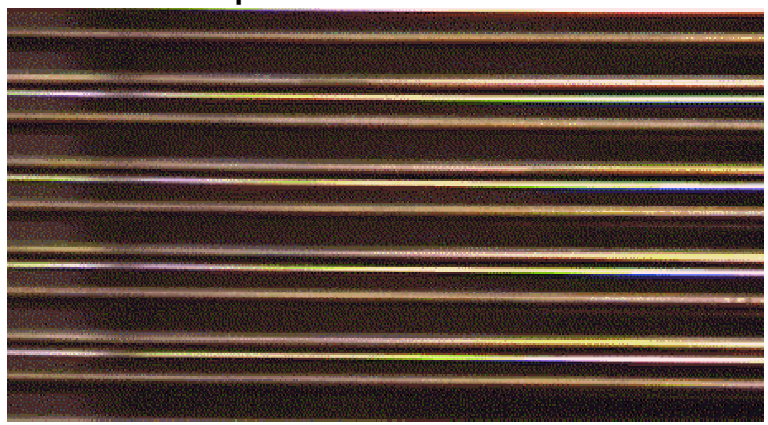

250 frames per second

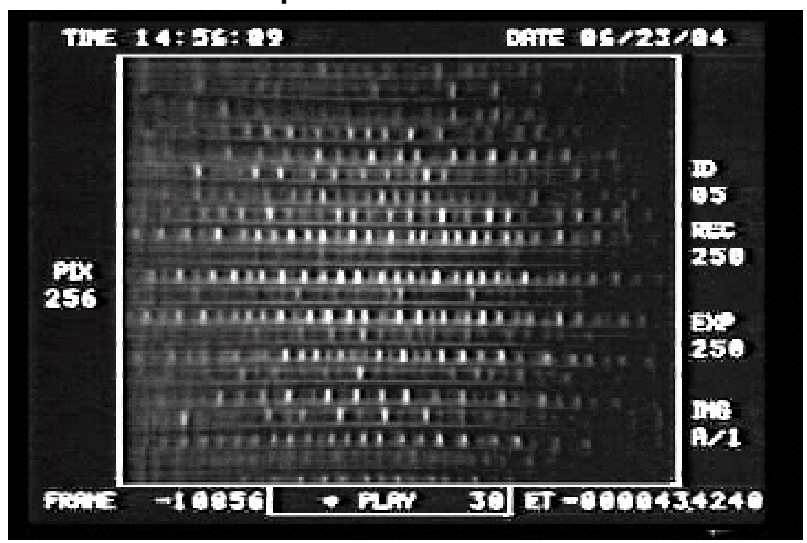

High speed camera

Microdischarge Patterning (2D)

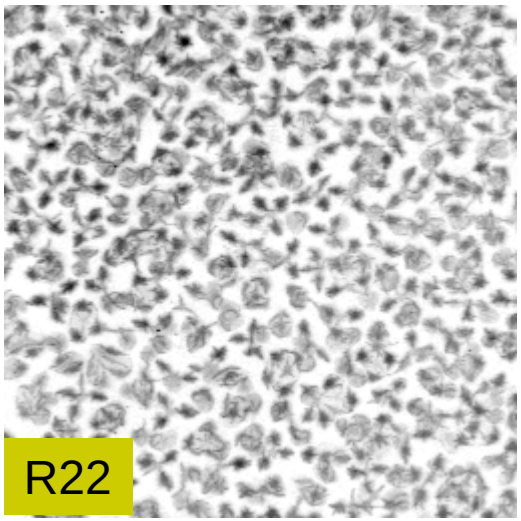

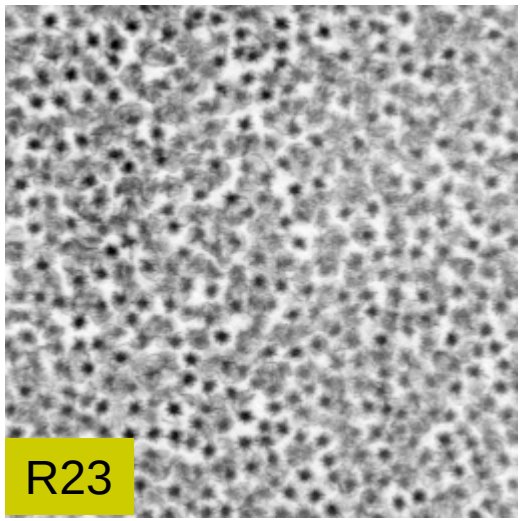

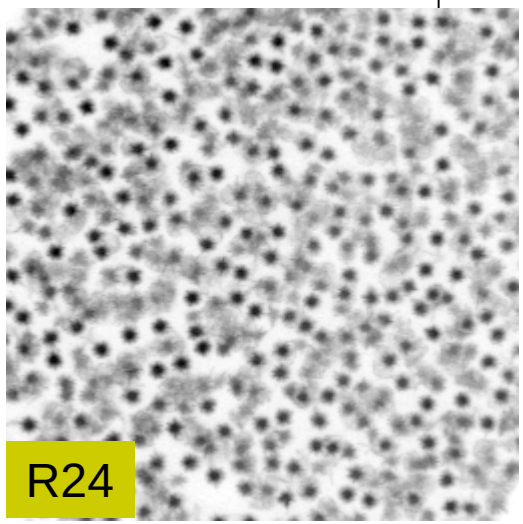

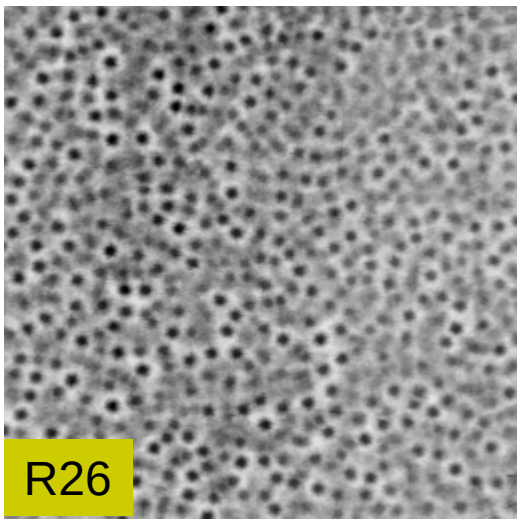

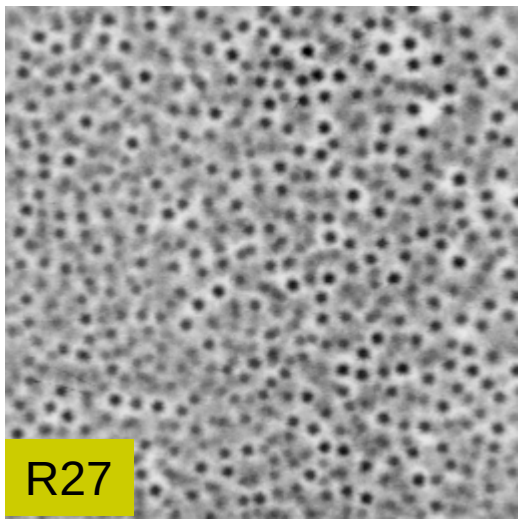

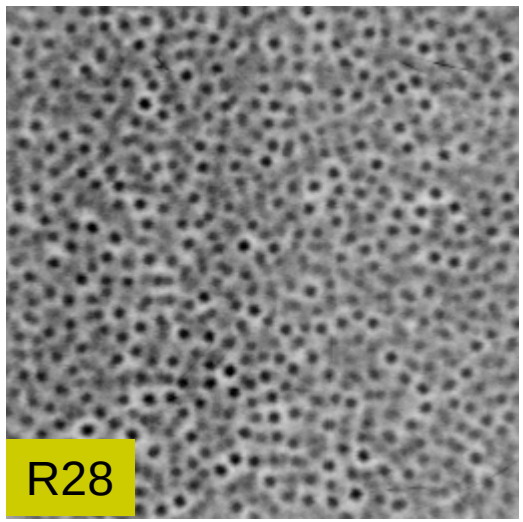

Discrete Fourier Transform (DFT) of Experimental Microdischarge Patterns

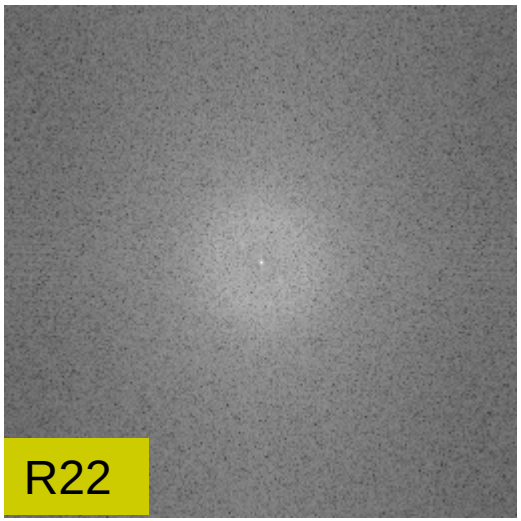

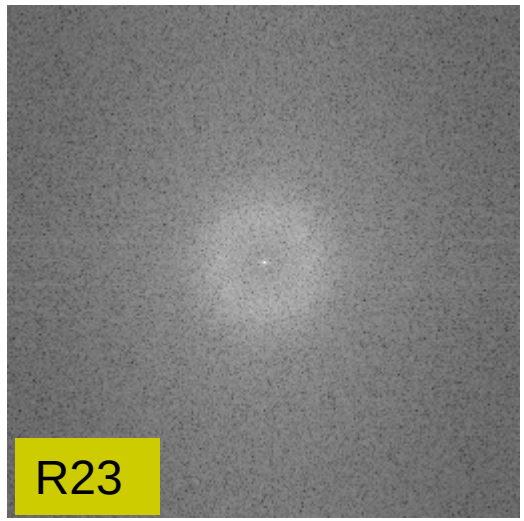

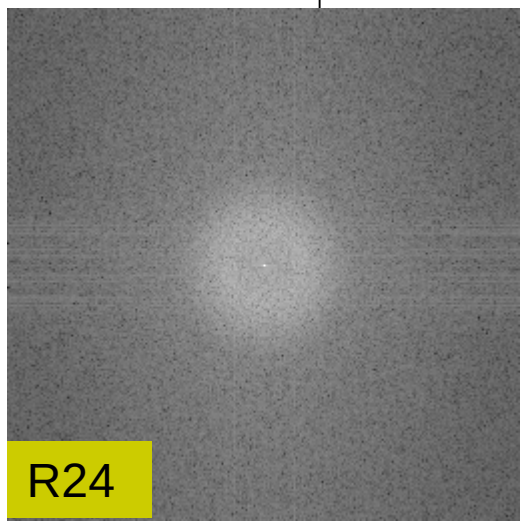

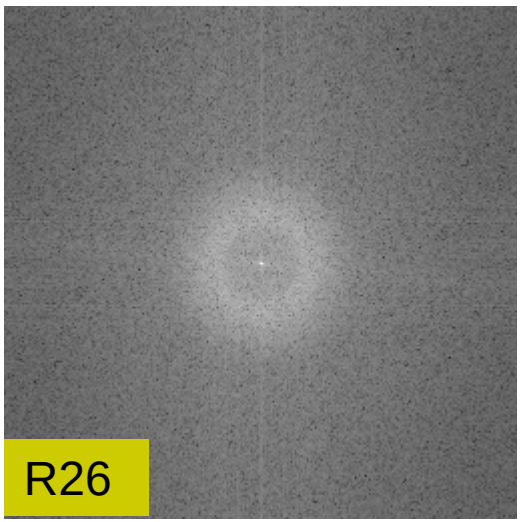

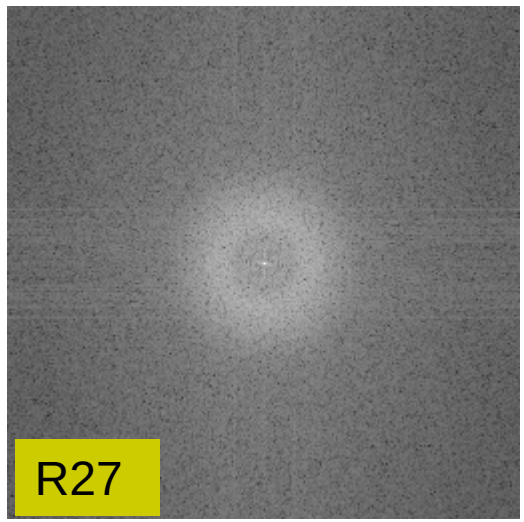

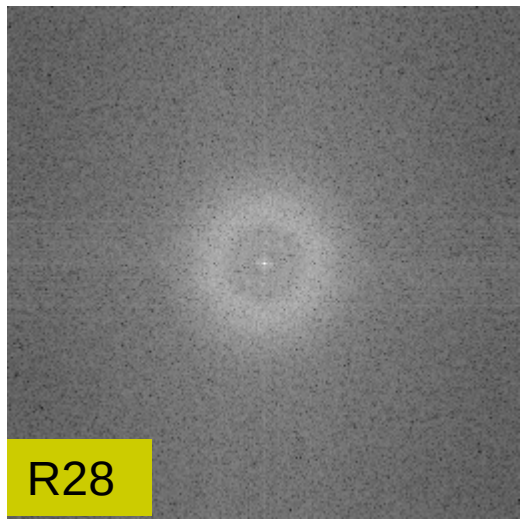

Microdischarge Patterning (2D)

Identified positions of the microdischarges

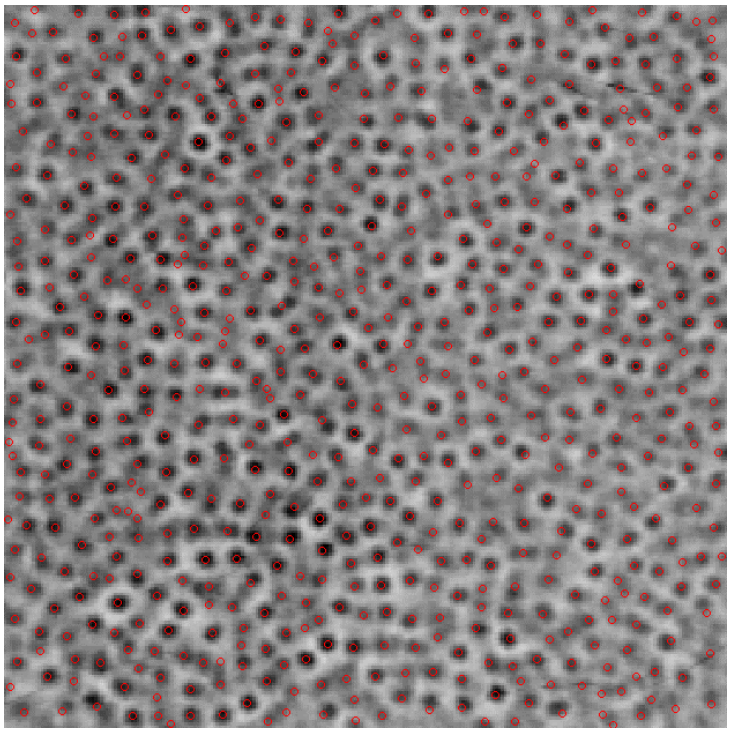

Voronoi Polyhedra constructed on identified microdischarges

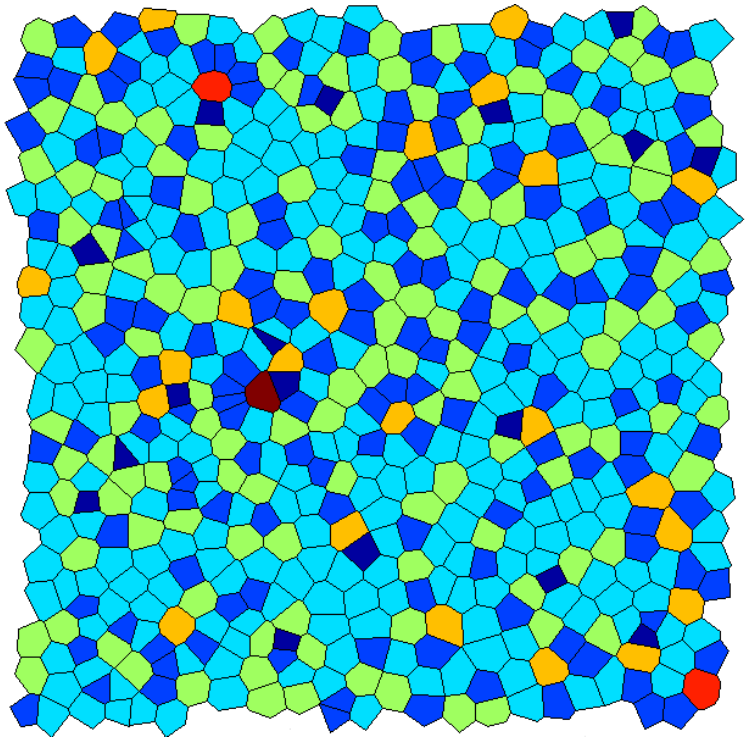

R28 used here as an example, this procedure was applied to all images

Microdischarge Patterning (2D)

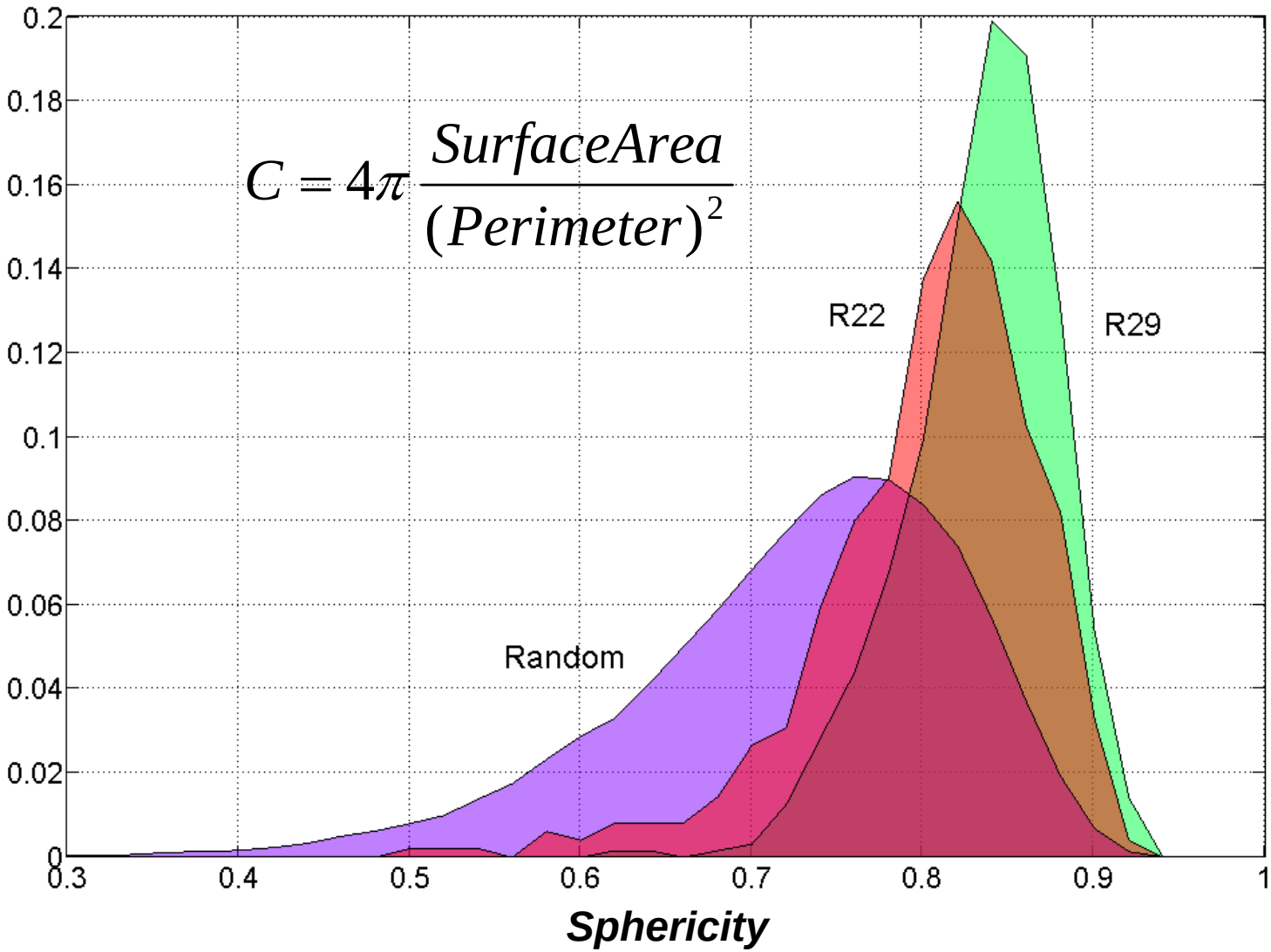

Influence of Microdischarge Interaction on Avalanche-to-Streamer Transition (Non-Continuous Monte-Carlo Model)

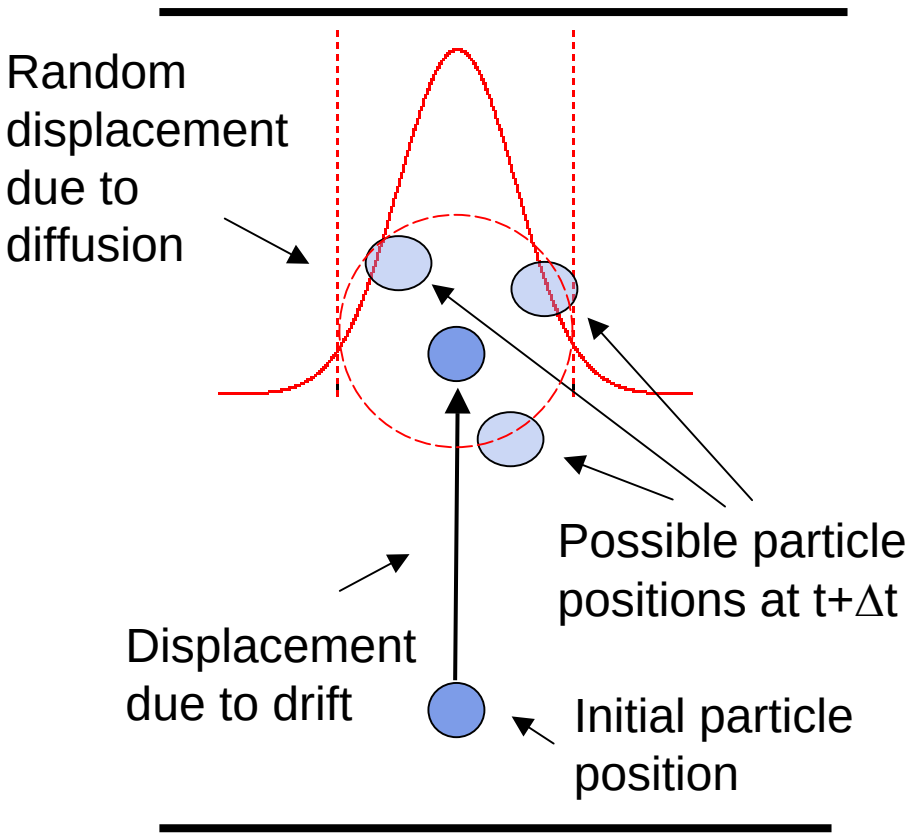

3D Non-Continuous Monte-Carlo Model of Avalanche:

Ionization and attachment are included in model, all other collisions are not Monte-Carlo considered.

Position of particle is calculated using displacement due to drift and random displacement due to diffusion.

Drift velocity and diffusion coefficient are function of local electric field. (local field approximation)

Model allows to simulates avalanche development in the discharge and measure statistical properties of avalanches.

Influence of Microdischarge Interaction on Avalanche-to-Streamer Transition (Non-Continuous Monte-Carlo Model)

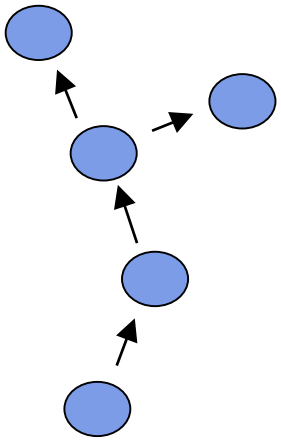

$$r(n) = \sum_{i=1}^{n} \eta(i), \quad \eta(i) \text{ - stochastic variable (normally distributed)}$$

$$E[r^2(n)] = n \cdot \sigma_\eta^2$$

$$\sigma_\eta^2 = 2 \cdot D \cdot \Delta t$$

Simulation of particle diffusion by Wiener process

Drift–Diffusion equation can be simulated be means of Wiener process.

Parameters of Wiener process are related to diffusion coefficient and mobility of the particle.

Brownian motion for clusters of many particles:

$$\sigma_{cluster}^2 = \frac{\sigma_\eta^2}{N}$$

Influence of Microdischarge Interaction on Avalanche-to-Streamer Transition (Non-Continuous Monte-Carlo Model)

3D Monte-Carlo simulation of series of 10 avalanches

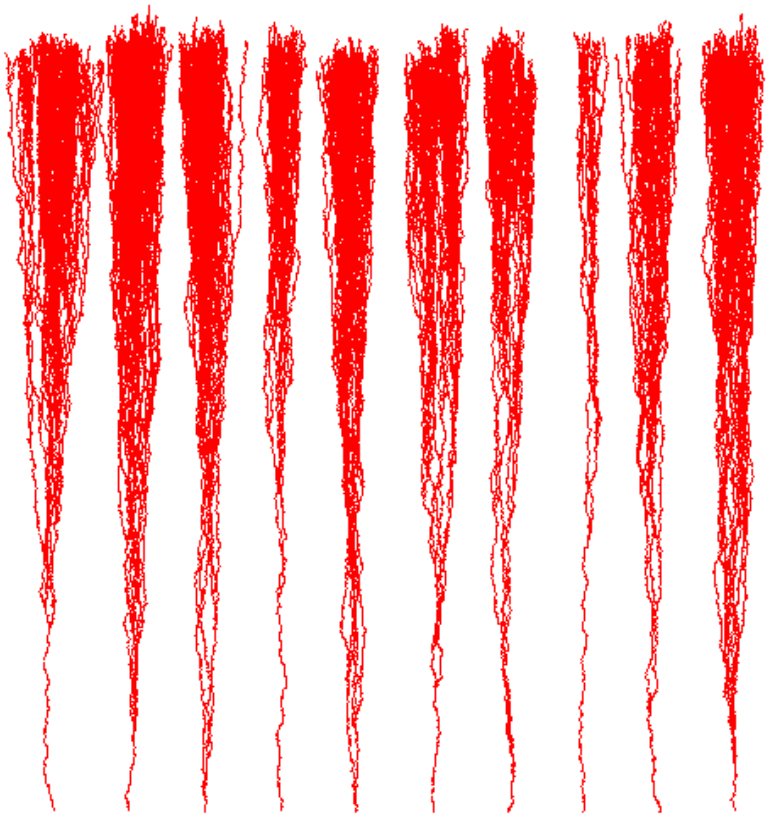

Average avalanche size is the same in both cases

$$\overline{N} = e^{(\alpha-\beta)\cdot d}$$

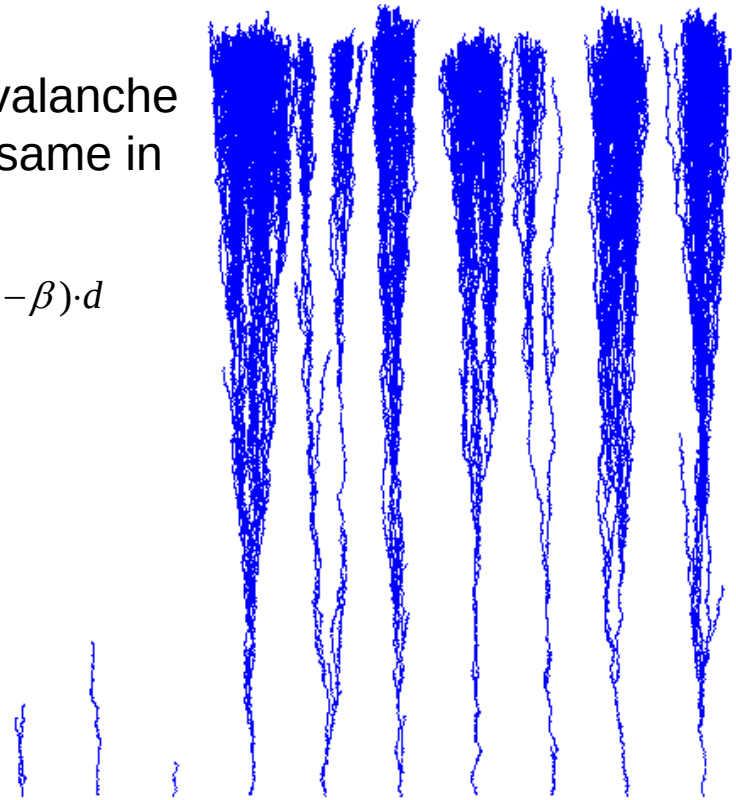

Non-electronegative gas: $\alpha d = 5$, $\beta d = 0$

electronegative gas: $\alpha d = 10$, $\beta d = 5$

Influence of Microdischarge Interaction on Avalanche-to-Streamer Transition (Non-Continuous Monte-Carlo Model)

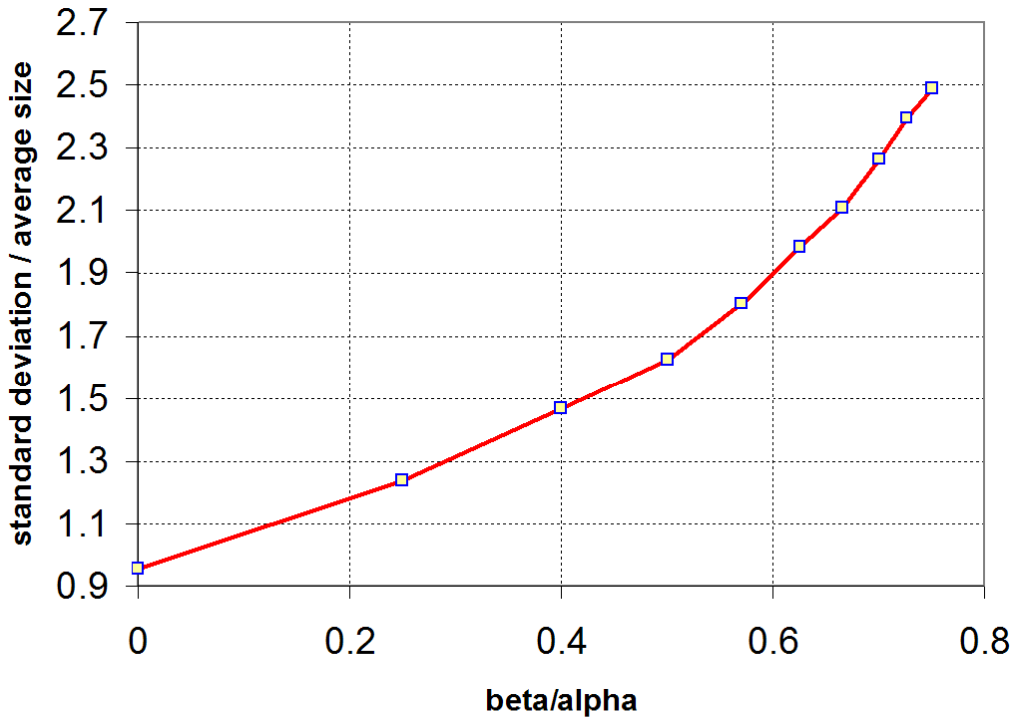

Standard deviation of the avalanche size from average is higher in the electronegative gas. Thus fluctuations of current are also higher.

Average avalanche size

$$\overline{N} = e^{(\alpha-\beta)\cdot d}$$

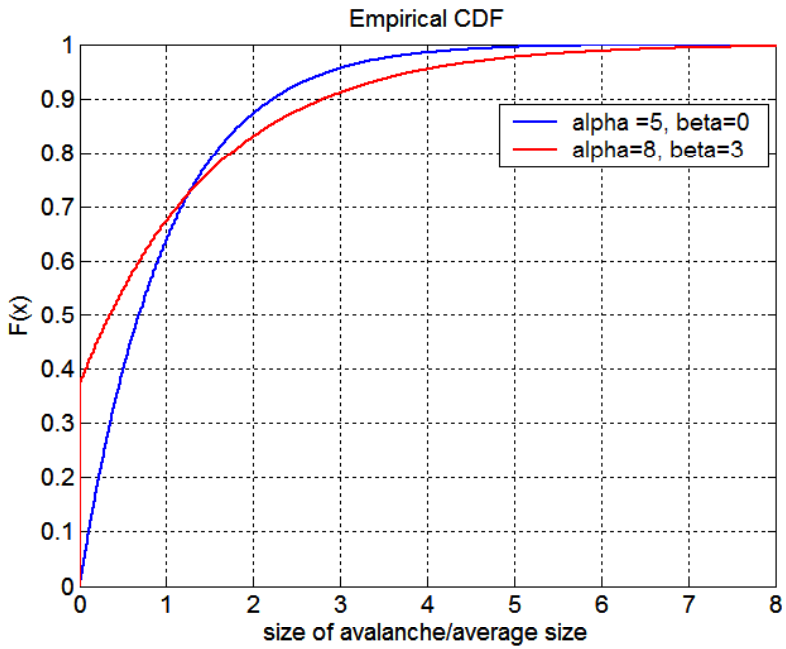

Cumulative distribution function of avalanche sizes.

Influence of Microdischarge Interaction on Avalanche-to-Streamer Transition (Meek Condition)

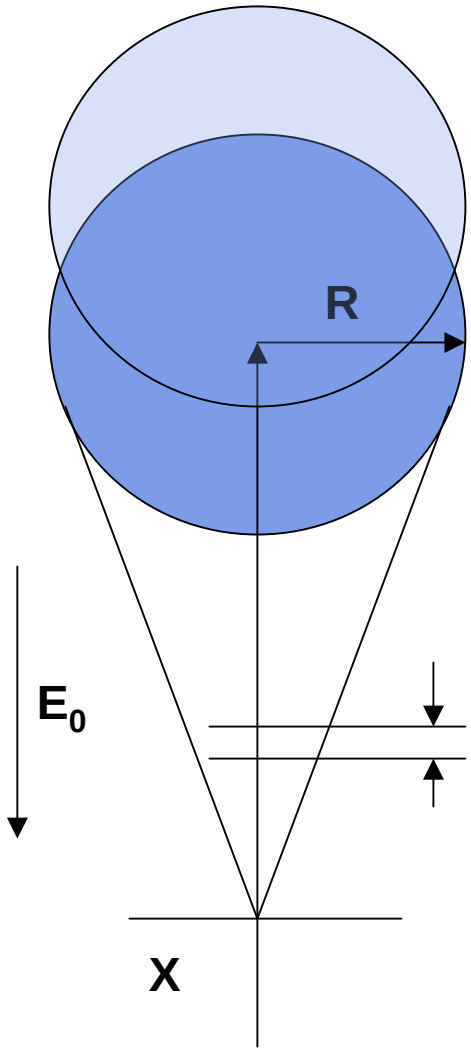

Meek condition for streamer formation

$$E = \frac{1}{4\pi\varepsilon_0}\cdot\frac{Q}{R^2} = \frac{1}{4\pi\varepsilon_0}\cdot\frac{n\cdot V\cdot\bar{e}}{R^2} = \frac{R\cdot n\cdot\bar{e}}{3\varepsilon_0}$$

$$E = \frac{\alpha\exp(\alpha x)\bar{e}}{3\pi R\varepsilon_0} \qquad R = \sqrt{2\cdot D\cdot x/V}$$

$$dN = d(\exp(\alpha x)) = \alpha\exp(\alpha x)dx$$

$$n = \frac{\alpha\exp(\alpha x)}{\pi R^2}$$

For 1 mm air gap at 1 atm: $\alpha d \approx 15.7$

Influence of Microdischarge Interaction on Avalanche-to-Streamer Transition (Modified Meek Condition)

Modified Meek condition for streamer formation: interacting avalanches

$$E = \frac{1}{4\pi\varepsilon_0}\cdot\left(\frac{Q}{R^2} - \frac{Q}{(L-R)^2}\right) = \frac{Q}{4\pi\varepsilon_0\cdot R^2}\cdot\left(\frac{1-2(R/L)}{(1-R/L)^2}\right)$$

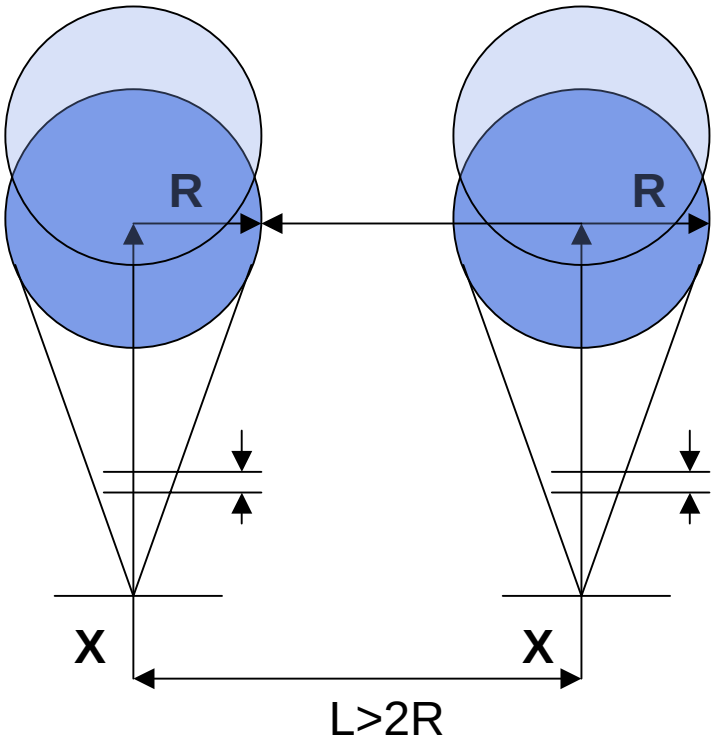

$$\frac{1-2(R/L)}{(1-R/L)^2} \approx 1-(R/L)^2$$

Modified Meek Condition:

$$\alpha d - (R/L)^2 \approx 15.7$$

Using pre-ionization density:

$$\alpha d \approx 15.7 + \sigma_e R^2$$


DREXEL
PLASMA
INSTITUTE
DARPA
Ben Franklin
Technology PArtners
Northeastern Pennsylvania
Non-Thermal Plasma
Blood Coagulation and
Sterilization of Surface Wounds

Plasma Medicine

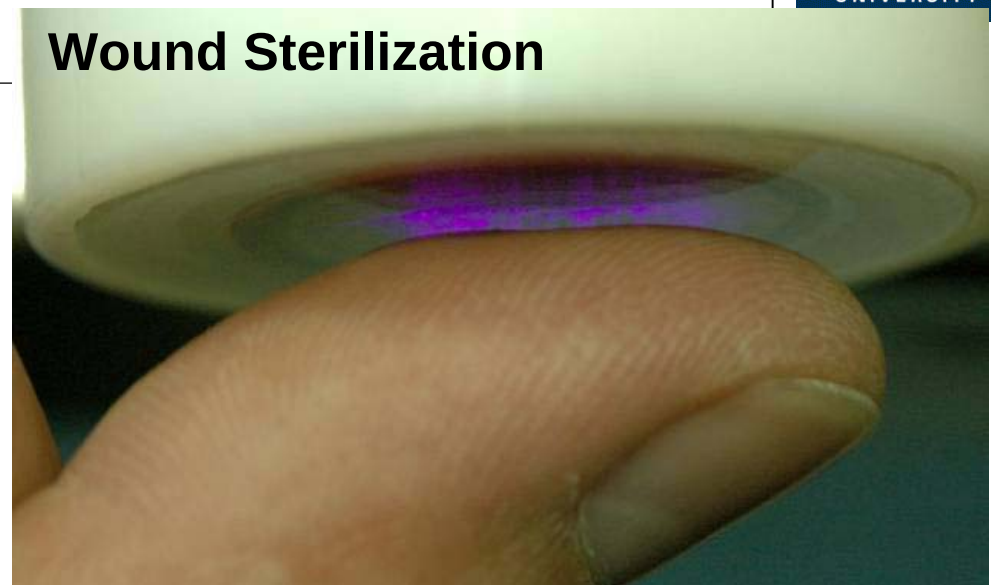

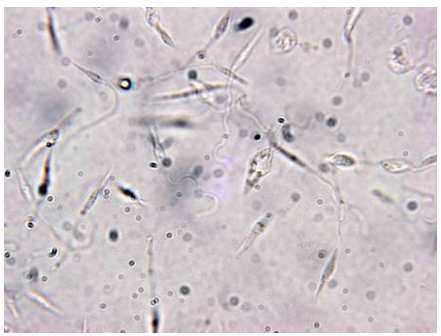

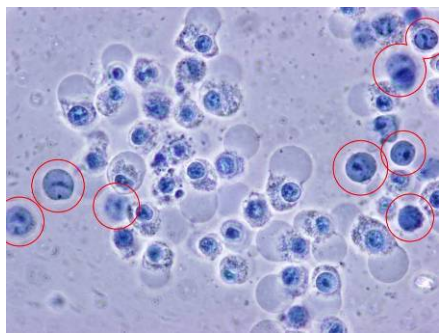

Treatment of Surface Wounds & Skin Diseases (Cutaneous Leishmaniasis)

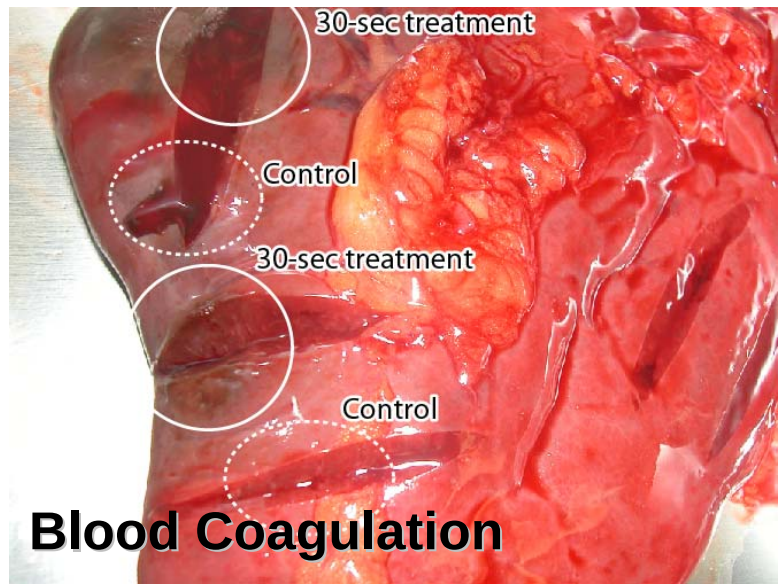

In-Vitro Blood Coagulation

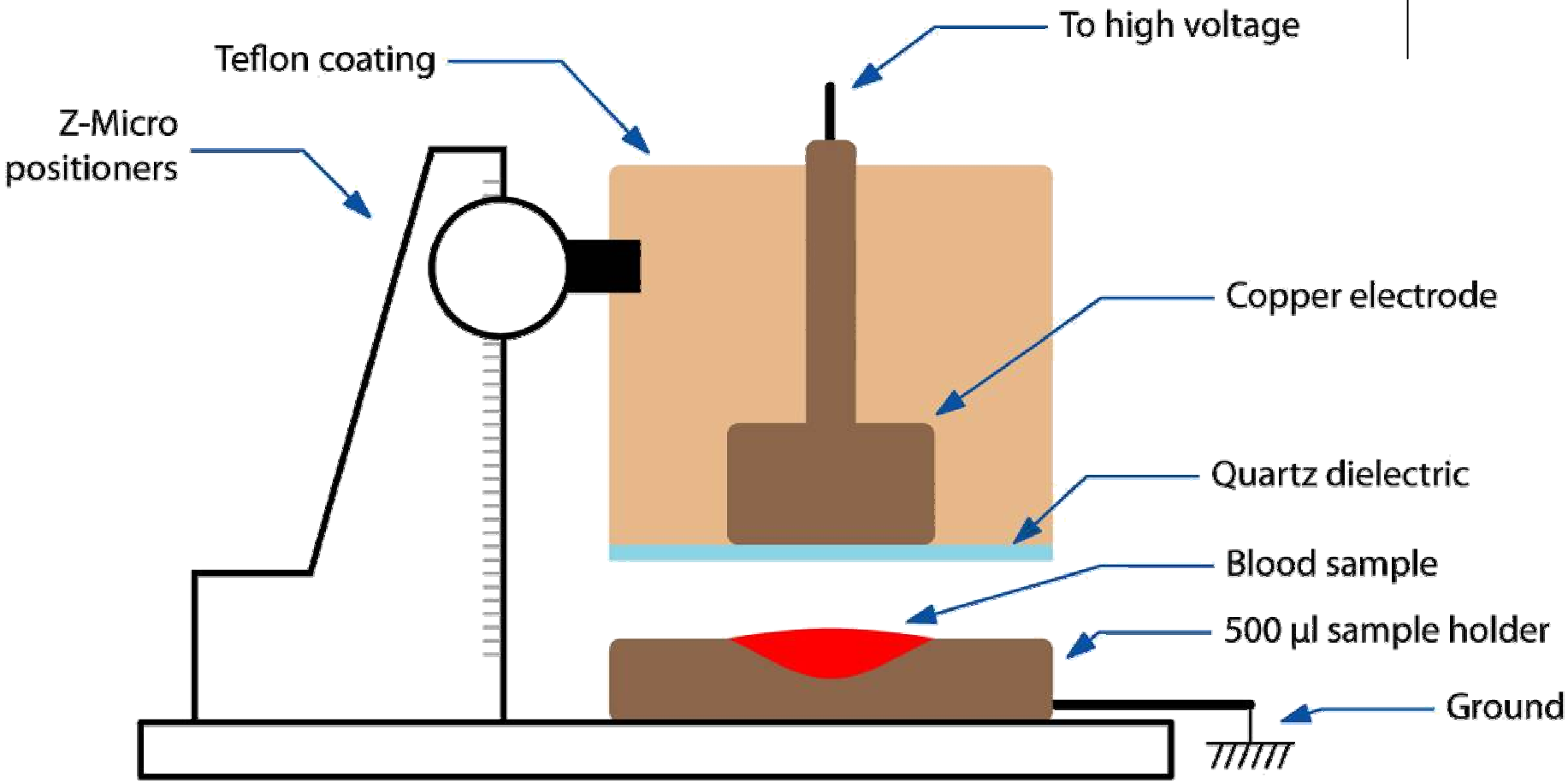

DBD: 12 KHz, 22KV, 1W/cm^2, Atmospheric air

In-Vitro Blood Coagulation

Gross/Visual examination:

Normal whole blood treated for 15 seconds completely coagulates in 2 minutes.

Untreated sample coagulates in 13 minutes

In-Vitro Blood Coagulation

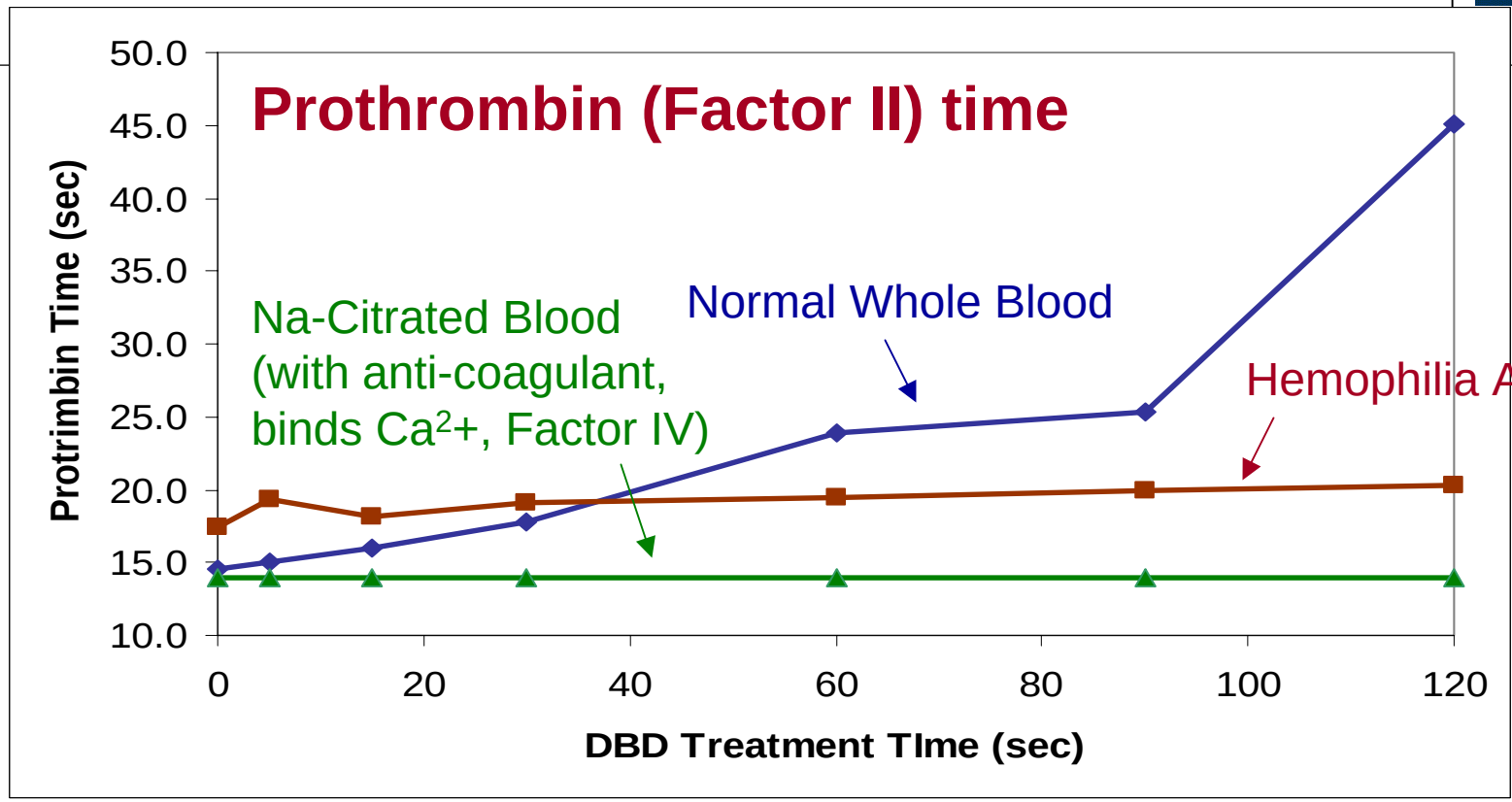

Prothrombin Time (PT) analysis:

Prothrombin (Factor II) time of residual blood increases 3 times after 120 seconds of DBD treatment.

Blood Coagulation Modeling

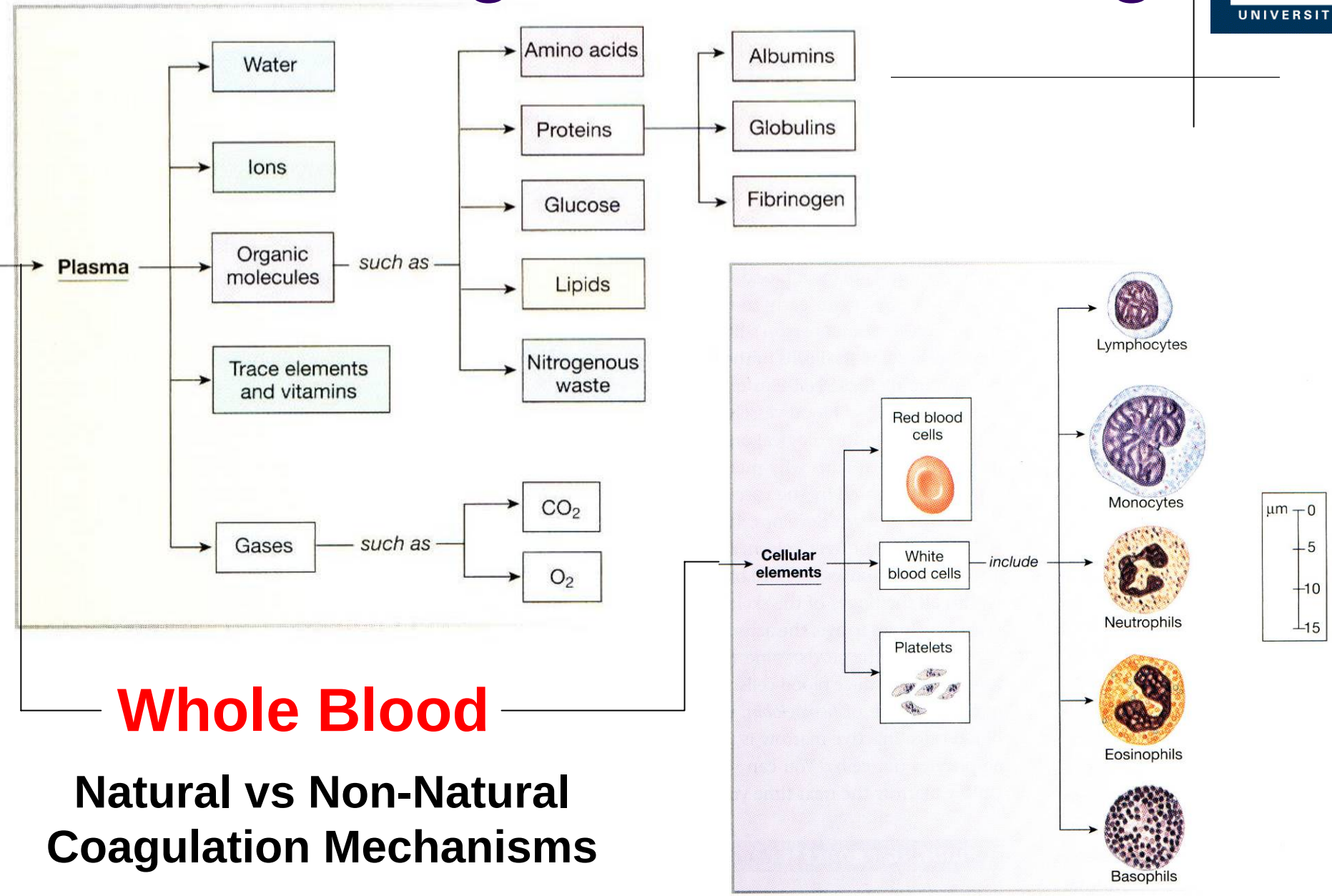

Whole Blood

Natural vs Non-Natural Coagulation Mechanisms

Blood Coagulation Modeling

Natural Coagulation Mechanism

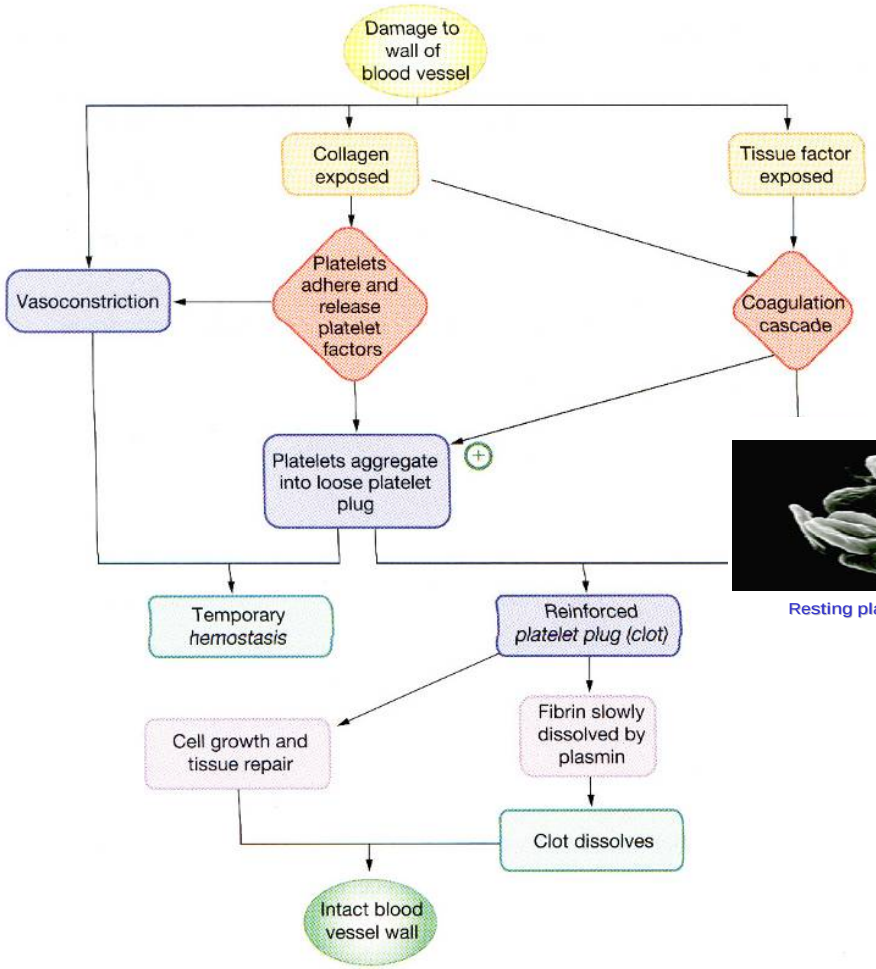

Coagulation Cascade

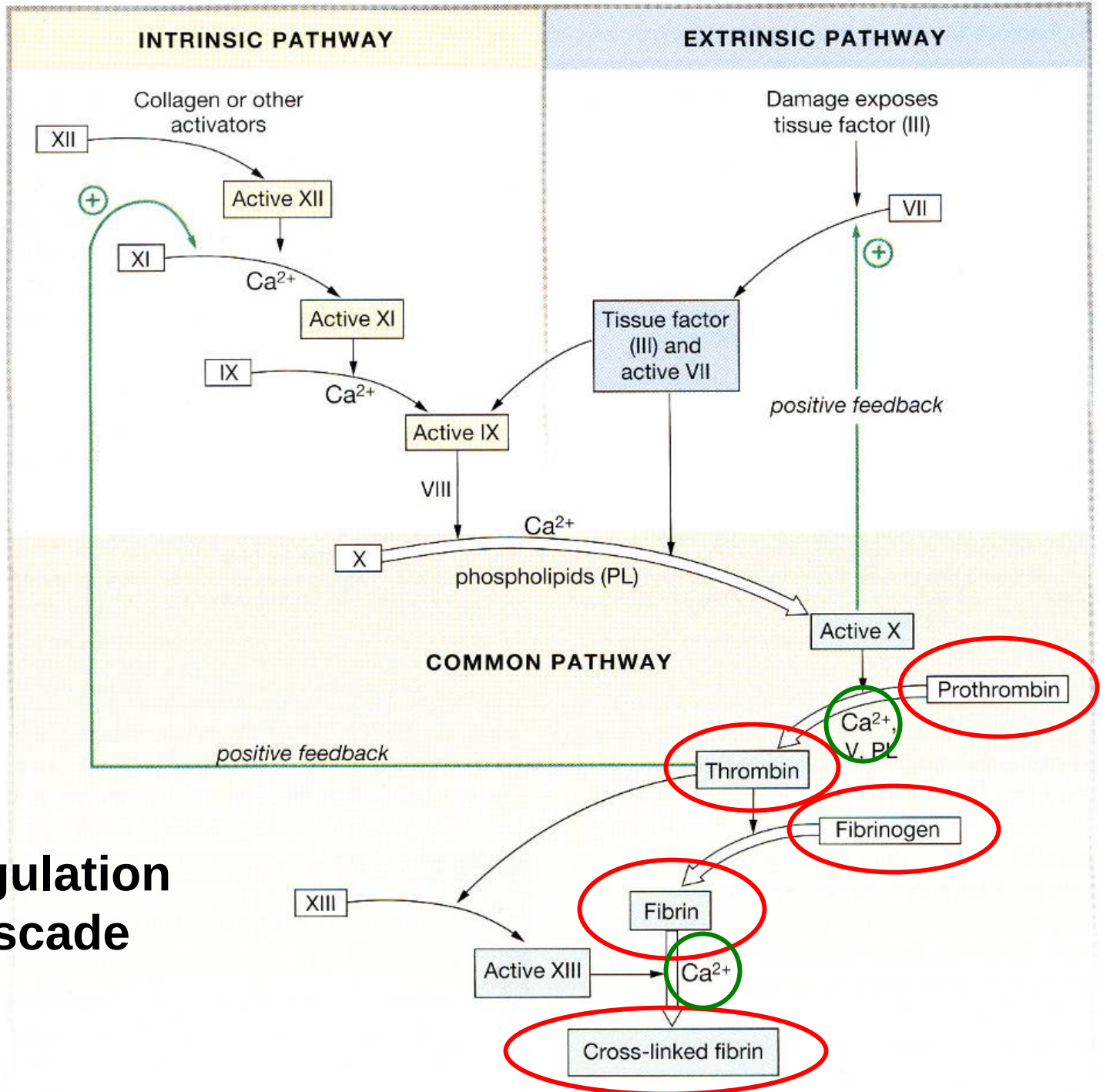

Blood Coagulation Modeling

(1) $IX + TF\text{-}VIIa \underset{k_{16}}{\overset{k_6}{\rightleftharpoons}} IX\text{-}TF\text{-}VIIa \xrightarrow{k_{11}} TF\text{-}VIIa + IXa$

(2) $X + TF\text{-}VIIa \underset{k_{17}}{\overset{k_5}{\rightleftharpoons}} X\text{-}TF\text{-}VIIa \xrightarrow{k_{12}} TF\text{-}VIIa + Xa$

(3) $X + VIIIA\text{-}IXa \underset{k_{18}}{\overset{k_5}{\rightleftharpoons}} X\text{-}VIIIa\text{-}IXa \xrightarrow{k_{11}} VIIIa\text{-}IXa + Xa$

(4) $IX + Xa \xrightarrow{k_{15}} Xa + IXa$

(5) $V + Xa \xrightarrow{k_1} Xa + Va$

(6) $VIII + Xa \xrightarrow{k_3} Xa + VIIIa$

(7) $V + IIa \xrightarrow{k_2} IIa + Va$

(8) $VIII + IIa \xrightarrow{k_4} IIa + VIIIa$

(9) $II + Va\text{-}Xa \underset{k_{19}}{\overset{k_5}{\rightleftharpoons}} II\text{-}Va\text{-}Xa \xrightarrow{k_{14}} Va\text{-}Xa + mIIa$

(10) $mIIa + Va\text{-}Xa \xrightarrow{k_8} Va\text{-}Xa + IIa$

(11) $VIIIa + IXa \underset{k_9}{\overset{k_7}{\rightleftharpoons}} VIIIa\text{-}IXa$

(12) $Va + Xa \underset{k_{10}}{\overset{k_8}{\rightleftharpoons}} Va\text{-}Xa$

Blood Coagulation Modeling

$$\left[Ca^{2+}R^{2-}\right] + H^{+}_{(H_2O)} \underset{k_{-Ca}}{\overset{k_{Ca}}{\rightleftharpoons}} \left[H^{+}R^{2-}\right]^{-}_{(H_2O)} + Ca^{2+}_{(H_2O)}$$

$$N_2^{+} + H_2O \xrightarrow{k_{gas}} N_2 + H_2O^{+}_{(H_2O)}$$

$$H_2O^{+}_{(H_2O)} + H_2O \xrightarrow{k_{ion}} H^{+}_{(H_2O)} + OH$$

Plasma generation of Ca^{2+} (Factor IV)

$$G_{N_2^+} = 0.3\ {}^{1}\!/_{100eV}$$

$$\Phi_{N_2^+} = G \cdot P = \left(0.3\ {}^{1}\!/_{100eV}\right) \cdot \left(1\ {}^{W}\!/_{cm^2}\right) =$$

$$= \left(0.3\ {}^{1}\!/_{100eV}\right) \cdot \left(\frac{1}{1.6 \cdot 10^{-19}}\ {}^{eV}\!/_{cm^2 \cdot sec}\right) \approx 2 \cdot 10^{16}\ \frac{N_2^+\ ions}{cm^2 \cdot sec}$$

$$OH + PlH \xrightarrow{k_{gas}} H_2O + Pl\bullet$$

$$Pl\bullet + PlO_2 \xrightarrow{k_{gas}} Pl\text{-}O\text{-}O\text{-}Pl$$

Phospholipid oxidation

Blood Coagulation Modeling

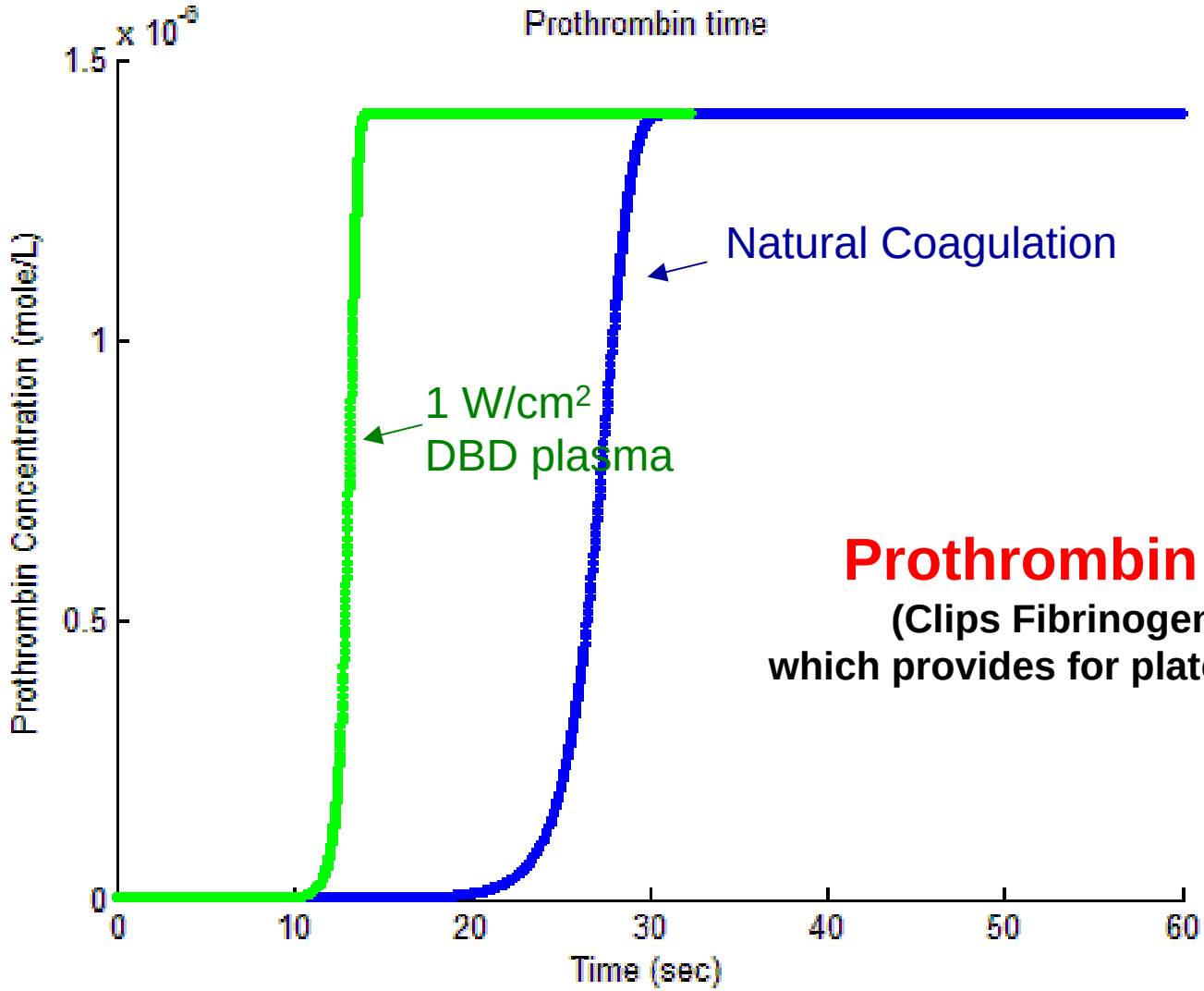

Prothrombin Kinetics

(Clips Fibrinogen to Fibrin, which provides for platelet aggregation)

“In-Vivo” Blood Coagulation

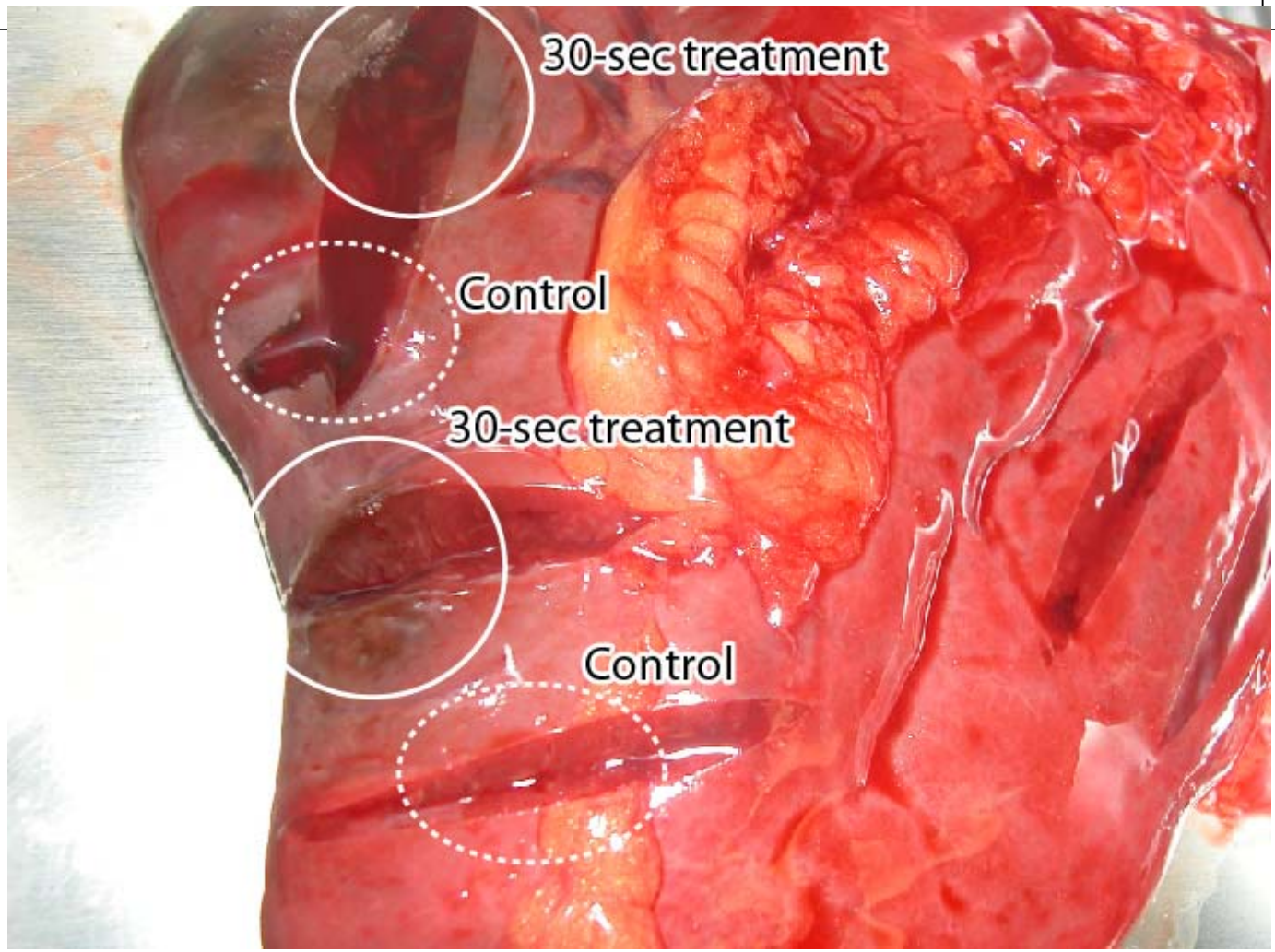

DBD Treatment of Spleen (cadaver tissue).

“In-Vivo” Blood Coagulation

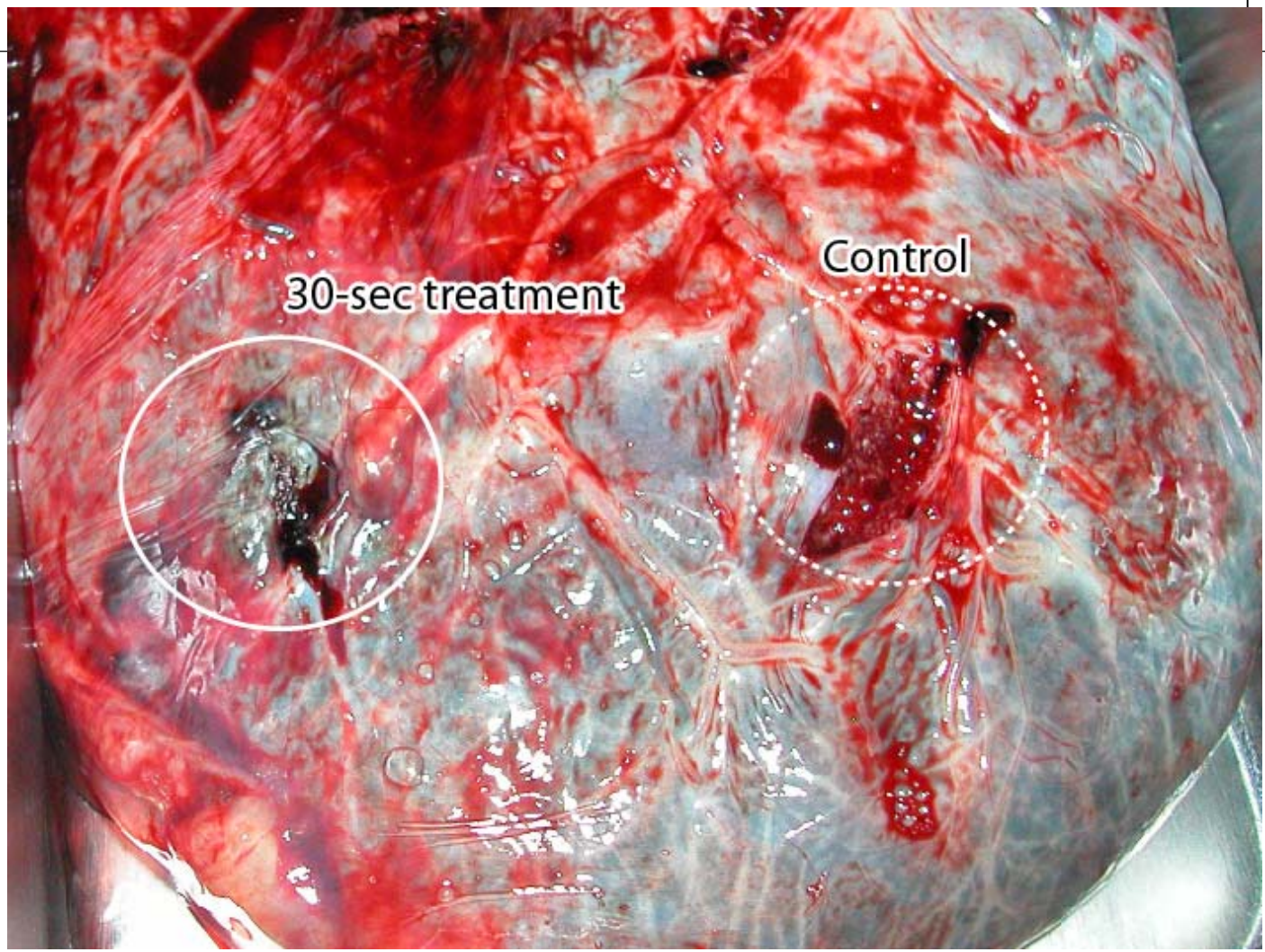

DBD Treatment of Placenta (explanted tissue).

“In-Vivo” Blood Coagulation

$$\overline{R}_p^{\Sigma} = \frac{i}{C_p\omega} + R_p$$

$$R_p^{\Sigma} = \sqrt{\left(\frac{1}{C_p\omega}\right)^2 + \left(R_p\right)^2}$$

$$R_h^{\Sigma} = \sqrt{\left(\frac{1}{C_h\omega}\right)^2 + \left(R_h\right)^2}$$

$$\sqrt{\left(\frac{1}{C_p\omega}\right)^2 + \left(R_p\right)^2} >> \sqrt{\left(\frac{1}{C_h\omega}\right)^2 + \left(R_h\right)^2}$$

Human: C_h=50 pF; R_h=1 MOhm;
Plasma: C_p=50 pF; R_p= 5 MOhm

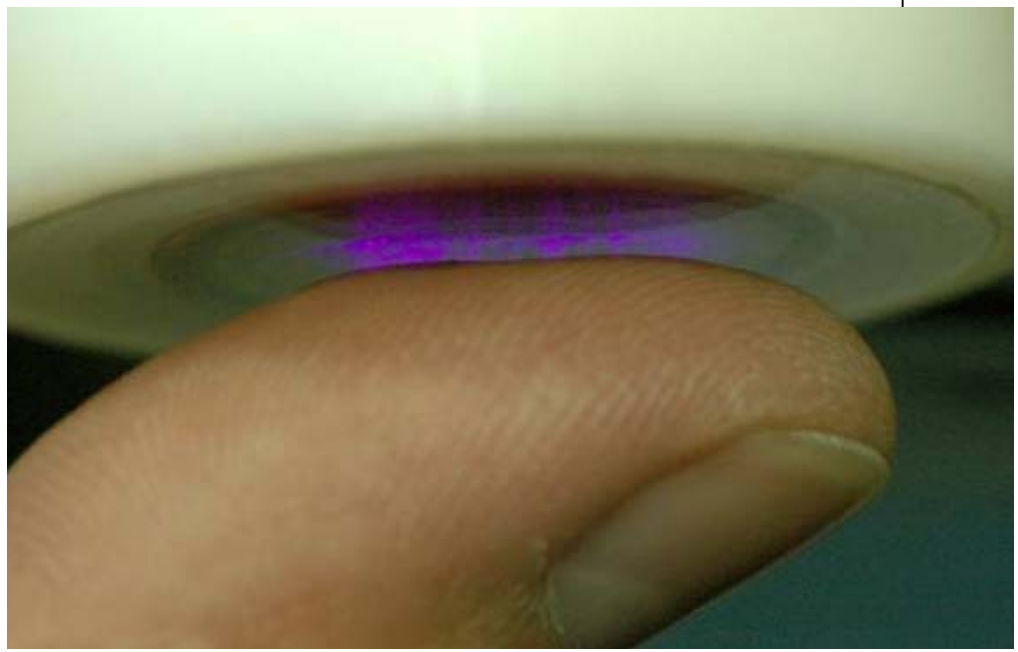

Total Resistance of a human: 1.9 MOhm
Total Resistance of DBD: 5-10 MOhm

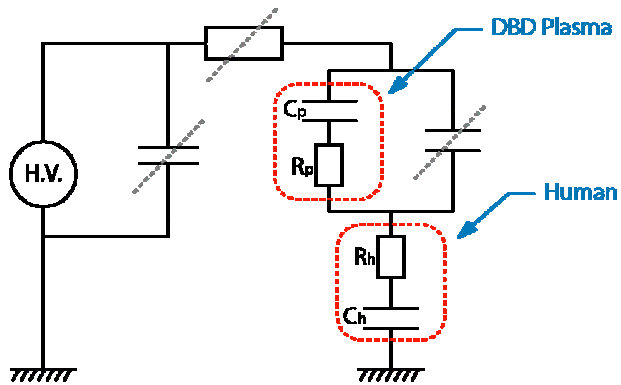

Tissue Sterilization Setup

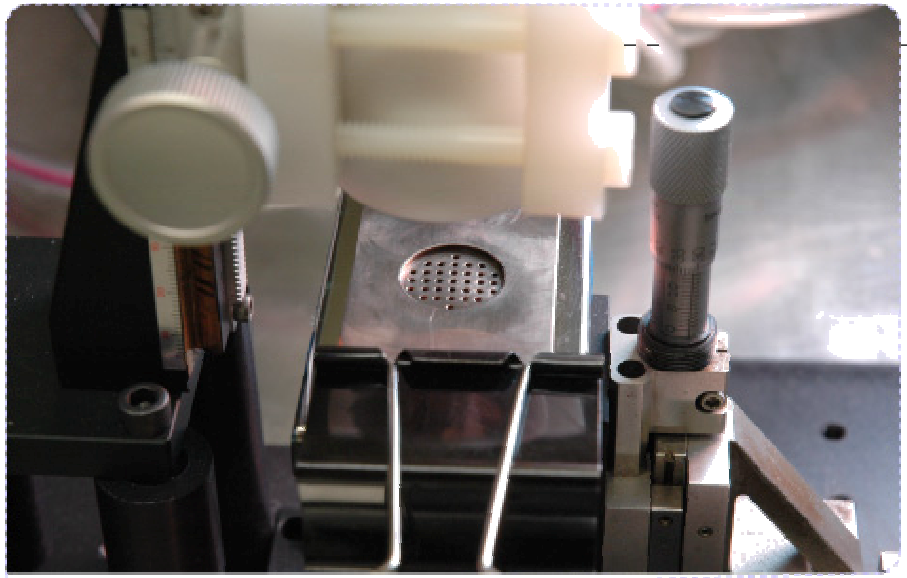

Tissue treatment setup

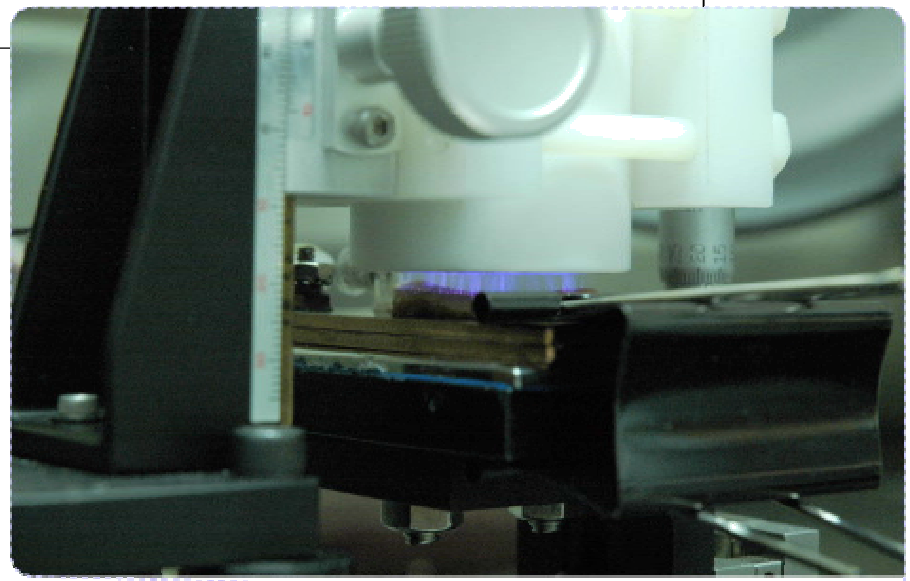

Tissue treatment by DBD plasma

DBD: 12 KHz, 22KV, 1W/cm^2, Atmospheric air

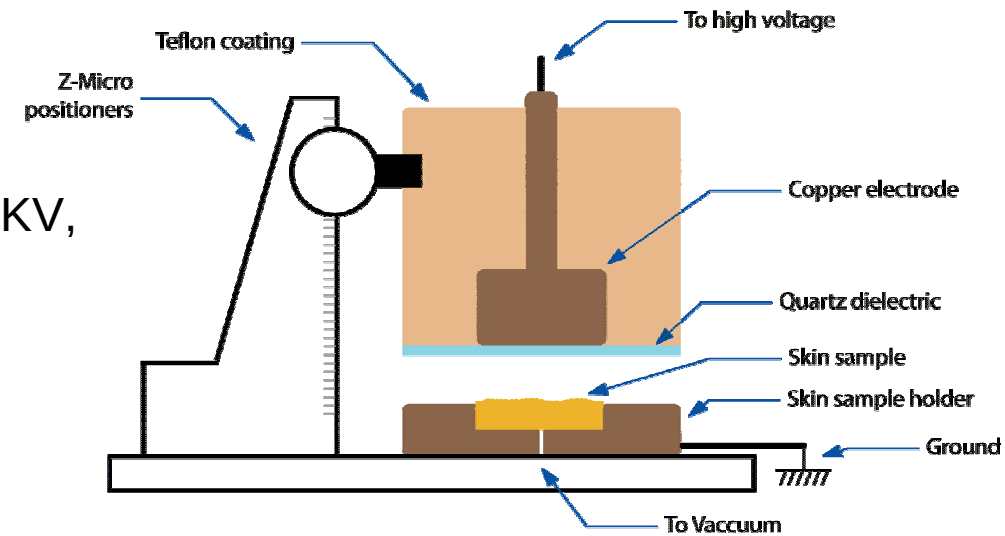

Tissue Sterilization

Before DBD Treatment

After 1-minute DBD Treatment

Complete sterilization in 4 seconds of DBD treatment from skin flora:

- **Streptococcus** (spherical gram-positive bacteria occurring in pairs or chains; cause e.g. scarlet fever and tonsillitis)
- **Staphylococcus** (spherical gram-positive parasitic bacteria that tend to form irregular colonies; some cause boils or septicemia or infections)
- **Yeast** (common name for an artificial assemblage of higher fungi which have temporarily or permanently abandoned the use of hyphal thalli; they are unicellular, and vegetative reproduction is generally by budding or fission)

No gross (visible) or microscopic tissue damage in up to 5 minutes of DBD treatment

Tissue sources: cadaver abdomen, leg, and arm skin, plastic surgery discards, wound tissue, and other tissue samples.

Tissue Damage Assessment

	BEFORE PLASMA TREATMENT	AFTER PLASMA TREATMENT	HISTOLOGY
CONTROL	 No treatment	N/A	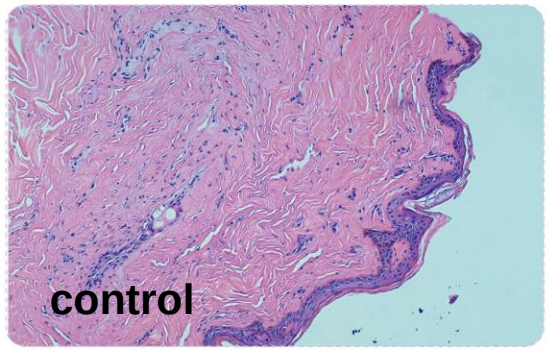 control
15 SECONDS	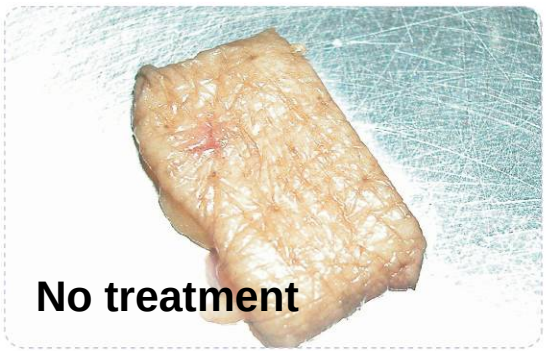 No treatment	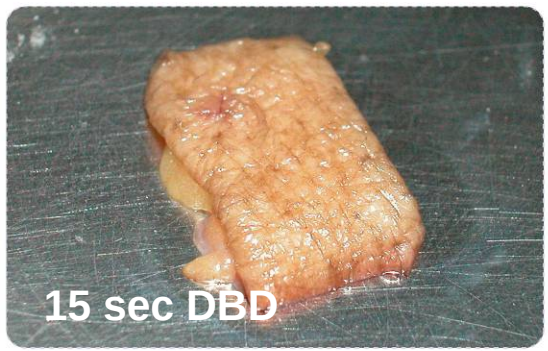 15 sec DBD	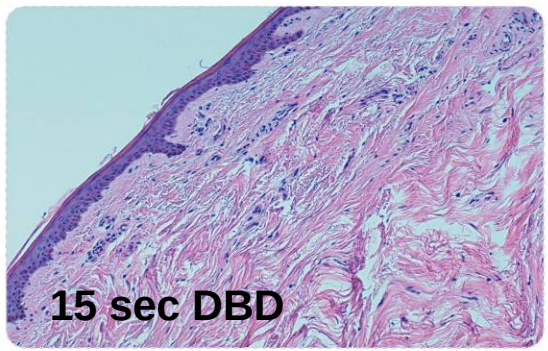 15 sec DBD
5 MINUTES	 No treatment	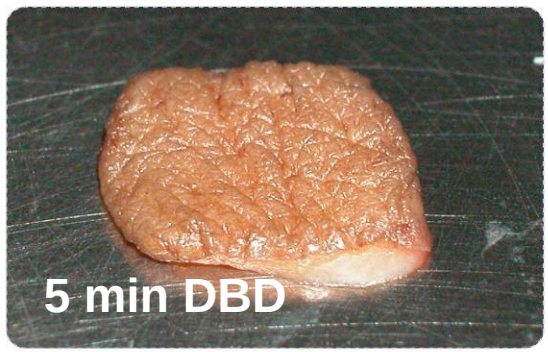 5 min DBD	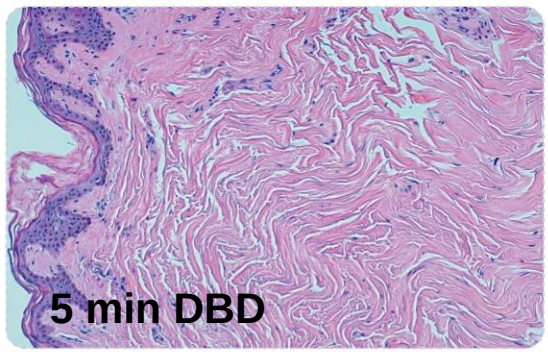 5 min DBD

Tissue Source: cadaver abdomen (stomach)

Sterilization Kinetic Modeling

Ozone Reactions with various bacteria	Inactivation Rate Coefficient in Air (cm^3/sec)	Inactivation Rate Coefficient in Water (cm^3/sec)
O_3 + Ecoli → Inactivated Ecoli	$6 \cdot 10^{-17}$	$2 \cdot 10^{-17}$
O_3 + Staphylococcus aureus (SA) → Inactivated SA	$2 \cdot 10^{-17}$	$2 \cdot 10^{-17*}$
O_3 + Fusarium oxysporum (FO) → Inactivated FO	$1 \cdot 10^{-16}$	$1 \cdot 10^{-16*}$
O_3 + S. Epidermis (SE) → Inactivated SE	$1 \cdot 10^{-15}$	$1 \cdot 10^{-15*}$
O_3 + Streptococcus salivarius (SSl) → Inactivated SSl	$4 \cdot 10^{-17}$	$4 \cdot 10^{-17*}$
O_3 + Rhizopus stolonifer (RS) → Inactivated RS	$2 \cdot 10^{-17}$	$2 \cdot 10^{-17*}$
O_3 + Serratia spp. (SS) → Inactivated SS	$1 \cdot 10^{-17}$	$1 \cdot 10^{-17*}$
O_3 + Proteus → Inactivated Proteus	$1 \cdot 10^{-17}$	$1 \cdot 10^{-17*}$
O_3 + Bacillus Megaterium (BM) → Inactivated BM	$2 \cdot 10^{-15*}$	$2 \cdot 10^{-15}$
O_3 + Mycobacterium fortuitum (MF) → Inactivated MF	$3 \cdot 10^{-15*}$	$3 \cdot 10^{-15}$
O_3 + Leuconostoc Mesenteroides (LMs) → Inactivated LMs	$4 \cdot 10^{-15*}$	$4 \cdot 10^{-15}$
O_3 + Listeria Monocytogenes (LM) → Inactivated LM	$7 \cdot 10^{-15*}$	$7 \cdot 10^{-15}$
AVERAGE	$\sim 10^{-16}$	$\sim 10^{-16}$

Sterilization Kinetic Modeling

Streptococcus inactivation by Plasma Ozone ($8*10^{15}$ cm^{-3})

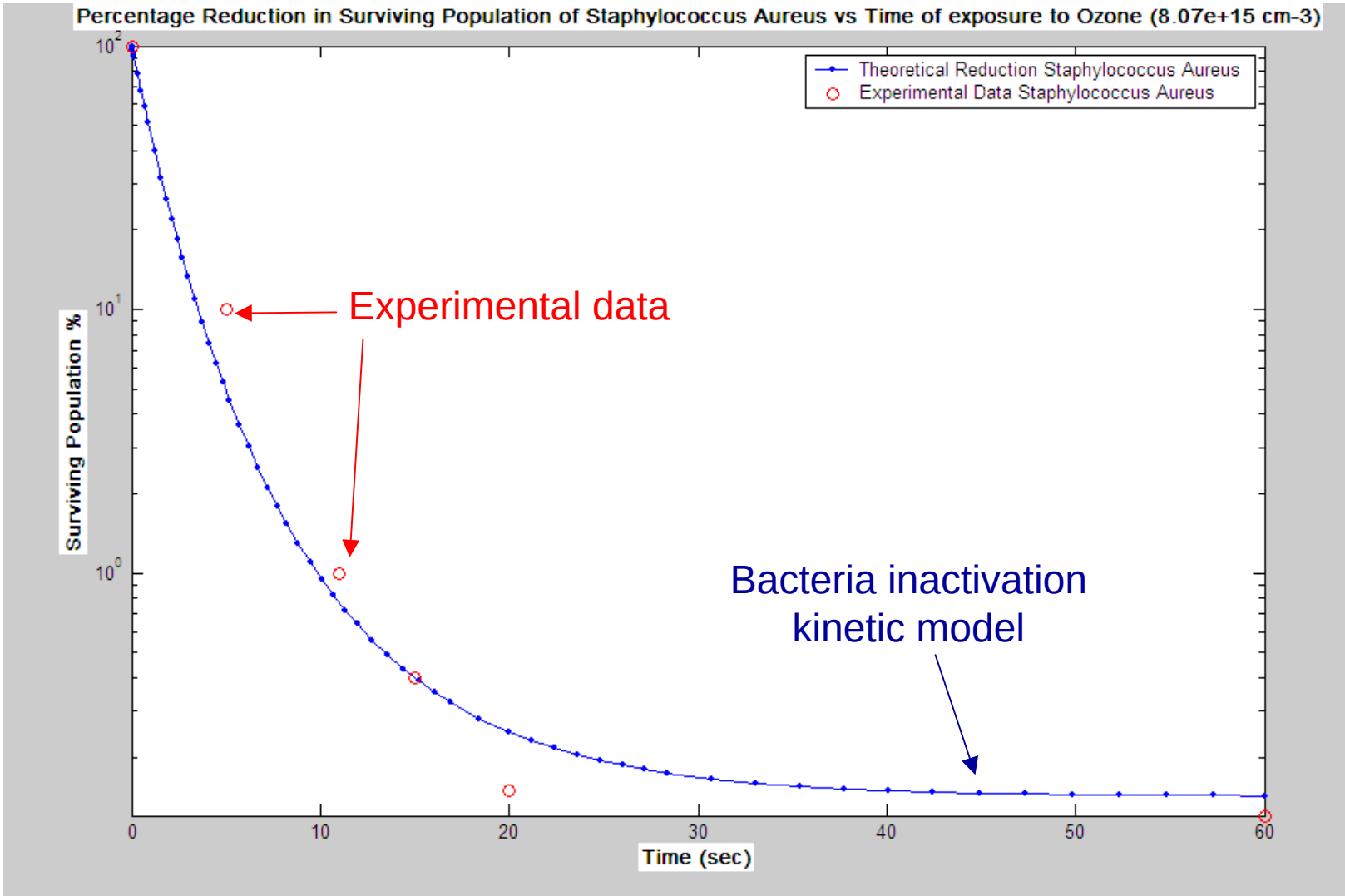

Sterilization Kinetic Modeling

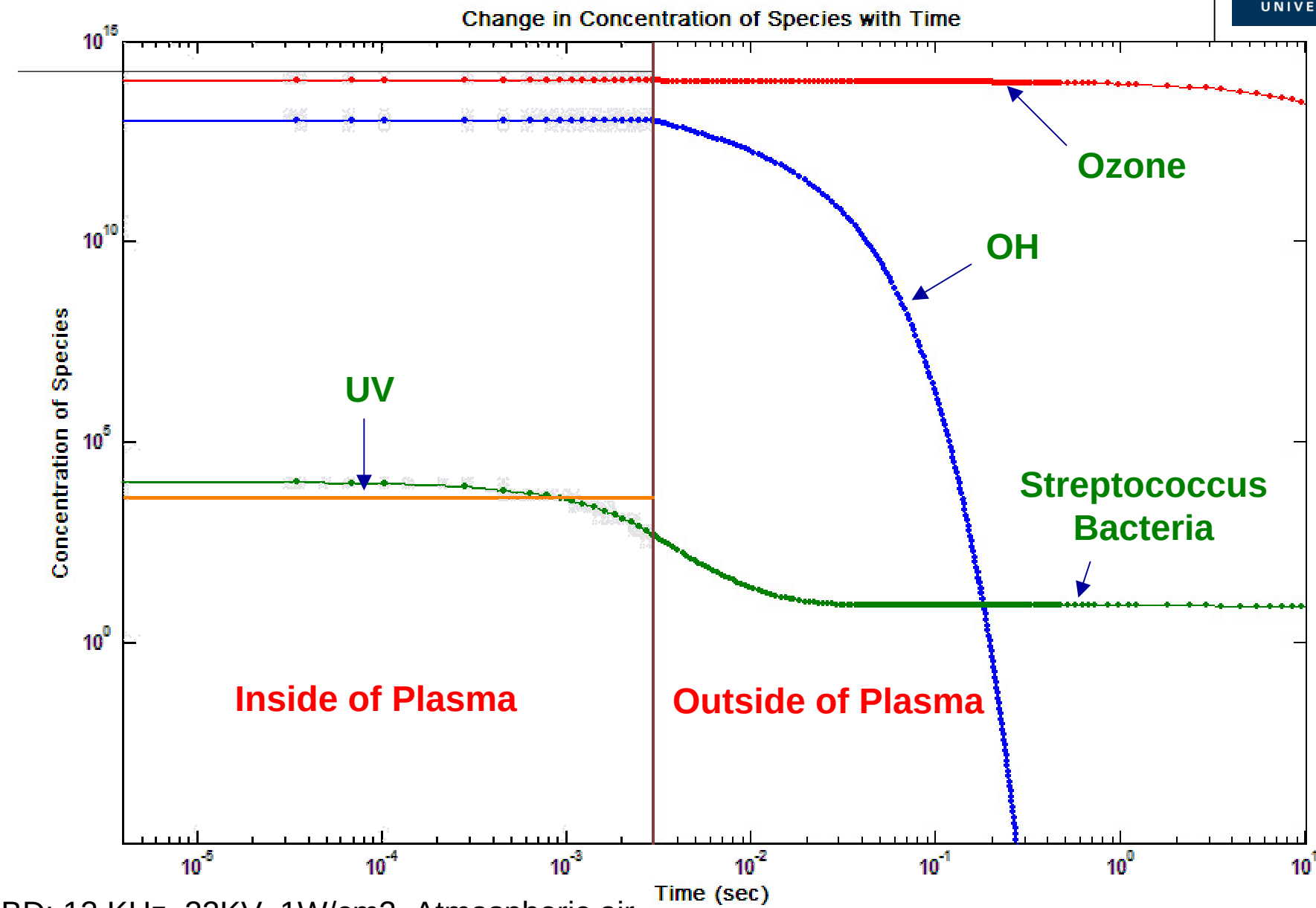

DBD: 12 KHz, 22KV, 1W/cm2, Atmospheric air

Drexel Plasma Institute